J Indian Inst Sci., Jan–Feb. 1991, 71, 53–89.

IISc THESES ABSTRACTS

Thesis Abstract (Ph.D.)

Standardization, immunochemical characterization, cross-reactivity and HLA-association of *Parthenium* pollen allergens by P. Sriramarao.
Research supervisor: P. V. Subba Rao.
Department: Biochemistry.

1. Introduction

The South American weed, *Parthenium hysterophorus* (American feverfew), a member of the Compositae family, was accidentally introduced into India around 1965 and has successfully colonized itself in several parts of the country[1]. Being an alien weed, its uninhibited growth is causing great concern. Studies carried out in our laboratory confirmed that the weed is responsible for allergic contact dermatitis. In addition, the pollen of this weed is established as an etiologic agent for allergic rhinitis.

2. Experimental and discussion

A detailed survey of the atmospheric pollens in Bangalore revealed that *Parthenium* pollen is wind borne and accounts for 48% of the total pollen count during the months of June-September which are favourable periods for the luxuriant growth and flowering of *Parthenium*[2]. In view of the increased incidence of allergic rhinitis during the past decade in Bangalore, the following studies on the prevalence of *Parthenium* rhinitis, standardization, immunochemical characterization, cross-reactivity and HLA-association of *Parthenium* pollen allergens were carried out.

A random clinical survey was conducted on 2035 residents of Bangalore city[3]. Allergy skin tests and questionnaire revealed that 7·1% of the study population was suffering from allergic rhinitis attributable to the pollen of *Parthenium hysterophorus*. *Parthenium* pollen-specific IgE and IgG antibodies were demonstrable in the sera of *Parthenium*-sensitive rhinitis patients by AB-microELISA and the specificity of these antibodies was established by ELISA-inhibition experiments. The presence of sensitized lymphocytes in *Parthenium* rhinitis patients was demonstrated by lymphocyte transformation experiments. To our knowledge, nowhere in the world has such a high incidence of allergic rhinitis due to a single pollen ever been reported.

The association of HLA-A, -B and -DR antigens with IgE-mediated *Parthenium* rhinitis was investigated[4]. A comparison of the phenotypic frequencies of HLA-A and -B antigens between *Parthenium* rhinitis patients and control subjects did not suggest any significant association. A significant correlation between HLA-DR_3 and *Parthenium* rhinitis with a relative risk of 11·33 was observed when compared to the control subjects.

A standardized in-house reference extract of *Parthenium* pollen has been generated by skin tests, RAST inhibition and isoelectric focussing[5]. *Parthenium*-reference allergen discs and positive reference

serum were also generated. These reference reagents were used for the quantitation of allergen-specific IgE in the sera of rhinitis patients and evaluation of relative potency of different batches of *Parthenium* pollen. A comparison of the composition and allergenic activity of the in-house reference extract with commercially available *Parthenium* pollen extracts (marketed in India by three different manufacturers for diagnosis and immunotherapy) revealed that the commercial preparations were of inferior quality, with very little allergenic activity.

Studies on the cross-reactivity of *Parthenium* and ragweed pollen allergens revealed that all the *Parthenium*-sensitive Indian patients never exposed to ragweed elicited positive skin reaction with extracts of ragweed pollen[6]. A significant correlation in the RAST scores of *Parthenium* and ragweed-specific IgE was observed in the sera of *Parthenium*(Indian)- and ragweed(USA)-sensitive patients. RAST-inhibition experiments demonstrated that the binding of IgE antibodies in the sera of ragweed-sensitive patients to ragweed allergen discs could be inhibited (up to 94%) by extracts of *Parthenium* pollen. Similarly, up to 82% inhibition in the binding of IgE antibodies to *Parthenium* allergen discs was observed when the sera of *Parthenium*-sensitive patients were preincubated with extracts of ragweed pollen. Immunoblot analysis demonstrated that the same major *Parthenium* and ragweed pollen allergens were recognized by the Indian and US sera.

Sera of patients with positive skin-prick reaction to *Parthenium* pollen extracts when analysed by ELISA revealed that 56·6 and 48·5% of the patients, respectively, had significant levels of *Parthenium*-specific IgE and IgG_4 antibodies[7]. Sixteen out of eighteen sera from patients with allergen-specific IgG_4 antibodies did not have any detectable levels of *Parthenium*-specific IgG_1, IgG_2, IgG_3 and IgE antibodies. Specificity of these IgG_4 antibodies was further confirmed by ELISA and immunoblot inhibition assays. IgG antibodies present in the sera of *Parthenium* rhinitis patients recognized the same major allergens as those recognized by IgE antibodies.

The major allergens of *Parthenium* pollen were found to be released very rapidly when extracted *in vitro*[8]. Although the extractable protein increased with time, all the soluble carbohydrate was released within 10 seconds of extraction. The allergenic activity of the rapid (10 seconds) and slowly (20 hour) released *Parthenium* pollen allergens was comparable by *in vivo* skin tests and ELISA-inhibition assay. The IEF patterns of the rapid and slowly released proteins were also identical. SDS-PAGE revealed that all the major pollen allergens (12, 31 and 52 K proteins) were eluted within 10 seconds of extraction. The results support the clinical observation of the rapid onset of symptoms of allergic rhinitis in patients sensitive to *Parthenium* pollen.

The major allergens of *Parthenium* pollen were purified by immunoaffinity chromatography using *Parthenium*-specific rabbit antibodies coupled to CNBr-activated Sepharose 4B. The affinity purified pollen proteins had comparable allergenic activity as those of the crude *Parthenium* pollen allergens. Purified allergens could totally inhibit the binding of the IgE and IgG antibodies to the immobilized allergens from crude extracts of *Parthenium* pollen. SDS-PAGE and immunoblot analysis revealed that all the major *Parthenium* pollen allergens (12, 31 and 52 K) were isolated by affinity chromatography.

References

1 Towers G. H. N., Mitchell, J. C., Rodriguez, E., Bennett, F. and Subba Rao, P. V. — Biology and chemistry of *Parthenium hysterophorus* L. A problem weed in India (Review), *J. Sci. Ind. Res.*, 1977, **36**, 672–684.

2 Mangala Seetharamaiah, A., Viswanath, B. and Subba Rao, P. V. — Atmospheric survey of pollen of *Parthenium hysterophorus*, *Ann. Allergy*, 1981, **47**, 192–196.

3 SRIRAMARAO, P., NAGPAL, S., SUBBA RAO, B. S., OM PRAKASH AND SUBBA RAO, P. V.	Immediate hypersensitivity to *Parthenium hysterophorus* II. Clinical studies on the prevalence of *Parthenium* rhinitis. *Clin. Expl Allergy*, 1991 (in press).
4. SRIRAMARAO, P., SELVAKUMAR, B., DAMODARAN, C., SUBBA RAO, B. S., OM PRAKASH AND SUBBA RAO, P. V.	Immediate hypersensitivity to *Parthenium hysterophorus* I: Association of HLA antigens and *Parthenium* rhinitis. *Clin. Expl Allergy*, 1991, **20**, 555–560.
5 SUBBA RAO, P. V., SRIRAMARAO, P. AND SCHRODER, H.	Standardization and generation of an in-house reference extract of the pollen of *Parthenium hysterophorus* – a potent world wide allergen. *Allergologie*, 1989, **12**, 18.
6 SRIRAMARAO, P., SCHRODER, H. AND SUBBA RAO P. V.	Crossreactivity of *Parthenium* and ragweed pollen allergens. *New Engl. Reg. Allergy Proc.*, 1988, **9**, 298.
7 SRIRAMARAO, P., OM PRAKASH, HUSSIAN, R. AND SUBBA RAO, P. V	*Parthenium* pollen-specific IgE and IgG_4 antibodies in rhinitis patients. *Proc. 7th Inter. Congr Immunol.*, 1989, **78**, 34.
8 SRIRAMARAO, P., BETAGERE, N. R., KORI, R., VENKATRAMAN, G. AND SUBBA RAO, P. V.	Kinetic studies on the rapid and slowly released *Parthenium* pollen allergens. *XIV Int Congr. of Allergology Clin. Immun.*, Tokyo, 1991 (submitted)

Thesis Abstract (Ph.D.)

Microbial degradation of indole: Studies on 2,3-dihydroxybenzoic acid decarboxylase from *Aspergillus niger* by Ajith V. Kamath.
Research supervisor: C. S. Vaidyanathan.
Department: Biochemistry.

1. Introduction

Microorganisms possess ability to degrade an array of recalcitrant xenobiotics including aromatic compounds. Indole is one of the polycyclic N-aromatic compounds present ubiquitously. Indole and its derivatives are pollutants released into the environment through industrial effluent sewage[1]. They are toxic, mutagenic and in some cases cause extensive chromosomal aberrations[2]. Bacteria degrade indole *via* the intermediate formation of dihydroxyindole, isatin, anthranilate, salicylate, catechol and gentisate followed by ring cleavage[3]. In plants, both anthranil and anthranilate have been invoked as intermediates in the pathway. Plants produce *o*-aminobenzaldehyde, 3-hydroxyanthranilate and *o*-aminophenol as intermediates which are not observed in other systems[4,5]. In animals, the metabolism of indole is directed mainly towards detoxification and excretion, in which cytochrome P-450 plays a vital role[6]. There is hardly any information on the degradation of indole by fungi.

2. Experimental and discussion

Aspergillus niger, a versatile soil fungus, was used for the study of degradation of indole. There was inhibition in the growth of the fungus in the presence of low concentrations (0.005–0.02%) of indole. A significant decrease was observed in the mycelial yield even when 125–500 fold excess of glucose was present in the medium. The intermediates of the pathway, namely, indoxyl, N-formylanthranilate, anthranilate, DHBA and catechol were isolated from the spent medium and identified N-formylanthranilate deformylase, anthranilate hydroxylase, DHBA decarboxylase and catechol dioxygenase activities were demonstrated in cell-free extracts of the mycelia grown on

medium containing indole. The enzyme levels were monitored during the growth curve of the fungus and it showed that all the enzymes were induced within 5–8 h of growth. All these results enabled the pathway to be proposed for the degradation of indole *via* indoxyl → N-formylanthranilate → anthranilate → 2, 3-dihydroxybenzoate → catechol. This is the first report on the degradation of indole by a fungus.

The enzyme, DHBA decarboxylase, was induced in *A. niger* by precursors, substrate analogs and by the product of the enzyme reaction, catechol. Salicylate, gentisate and DHBA showed good induction. The minimal structural requirement for the induction was a hydroxyl group in *ortho* position to the carboxyl group on the benzene ring. The enzyme was purified using ammonium sulfate fractionation, DEAE-sephacel and affinity chromatography (prepared by coupling a competitive inhibitor, salicylate to benzidylsepharose). The homogeneity of the enzyme was established by polyacrylamide gel electrophoresis (PAGE). The enzyme had a molecular weight of 120,000 and SDS-PAGE showed a single band with a molecular weight of approximately 28,000 suggesting the native enzyme to be a tetramer of identical subunits. The enzyme did not require any cofactors for activity and was not inhibited by carboxyl reagents suggesting that the enzyme did not require a carboxyl group for activity. The enzyme was drastically inhibited by heavy metals like Hg^{2+} and Cd^{2+} and thiol reagents.

The DHBA decarboxylase had a fluorescence excitation maximum of 280 nm and emission maximum of 340 nm. When experiments were carried out with an extrinsic fluorescent probe, such as, 8-anilinonaphthalenesulfonic acid (ANS), there was an enhancement in the fluorescence of ANS, suggesting that it was binding at the hydrophobic pocket of the enzyme. The enzyme, pretreated with a competitive inhibitor, did not yield such an enhancement in the fluorescence of ANS suggesting that the substrate binding site might be hydrophobic in nature. The fluorescence enhancement experiment and the hydrophobic nature of the substrate of the enzyme suggested a possible role for a tryptophan residue at the active site.

Circular dichroism (CD) studies of DHBA decarboxylase in 205–250 nm region showed that the enzyme had significant amount of α-helix secondary structure. The CD spectrum in the near-UV region showed a broad band at 285 nm which might be due to the contribution of tryptophan and or tyrosine residues in the enzyme. When the enzyme was treated with denaturants, buffers of different pH values and substrate analogs, there was a change in the near-UV CD spectrum but not in the far-UV CD spectrum. This suggested the probable participation of aromatic side chain in substrate binding catalysis.

DHBA Decarboxylase was inhibited by substrate analogs especially by compounds containing a relatively small group, in *ortho* position to the carboxyl group on the benzene ring. Compounds with a hydroxyl group on C-3 were not inhibitors suggesting that the carboxyl and hydroxyl groups on C-2 are essential for interaction at the active site of the enzyme. The pK_a value for the amino-acid residue involved in enzyme reaction was determined to be 6.2 which corresponded well with the pK_a of histidine, implicating the participation of an imidazole moeity in the decarboxylation.

DHBA Decarboxylase was probed for the active-site amino acids using modification reagents specific for histidine, tryptophan and cysteine. Histidine residues in the enzyme were modified using diethylpyrocarbonate (DEPC) and the number of DEPC molecules required to inactivate one active centre was calculated to be 0.95 suggesting at least one histidine residue per active site. Substrate analogs and competitive inhibitors protected the enzyme against inactivation implying that the modification occurred probably at or near the active site. The modified inactive enzyme was reactivated to 90% by treatment with hydroxylamine suggesting that the amino acid modified was a histidine residue. This was further confirmed by the difference spectrum of the DEPC-treated enzyme which

showed a peak at 240 nm due to the formation of carvethoxy derivatives of histidine. Tryptophan residue was modified using N-bromosuccinimide. The modification experiments revealed the involvement of one tryptophan residue per active site of the enzyme. This was further supported by the protection experiments by substrate analogs. The involvement of a cysteine residue was suggested by the potent inhibition by thiol reagents and heavy metal ions. Cysteine residue was modified using N-ethylmaleimide. The modification and protection experiments revealed the presence of one cysteine per active site. In the protection experiments performed in the case of all three modification studies, aromatic compounds with a hydroxyl group or a small group at C-2 on the benzoic acid specifically protected the enzyme. Obtaining support from all these results, a possible mechanism for the decarboxylation of DHBA by the enzyme was proposed.

Immobilization studies were carried out using three inert matrices, namely, calcium alginate, polyacrylamide gel and agar, for the transformation of indole. The immobilized mycelia of *A. niger* were more efficient than the free mycelia. The fungus immobilized on calcium alginate and polyacrylamide could be used for 6–7 batches with rejuvenation. This work has a possible application in the treatment of industrial wastes and sewage water which contain indole derivatives.

References

1. ELLIS, D. D., JONE, C. M., LARSON, R. A AND SHAEFFER, D. — *Arch. Environ. Contamination Toxicol.*, 1982, **11**, 372–382.
2. WANG, C. Y. — *Mutation Res.*, 1977, **56**, 7–12
3. SAKAMOTO, Y., UCHIDA, M AND ICHIHARA, K — *Med. J. Osaka Univ.*, 1953, **3**, 477–486
4. NAIR, P. M. AND VAIDYANATHAN, C. S. — *Biochim. Biophys. Acta*, 1964, **81**, 496–506.
5. DIVAKAR, N. G., SUBRAMANIAN, V., SUGUMARAN, M. AND VAIDYANATHAN, C. S — *Pl. Sci. Lett.*, 1979, **15**, 177–181.
6. KING, L. J., PARKE, D. G. AND WILLIAMS, R. T — *Biochem. J.*, 1966, **98**, 266–277.

Thesis Abstract (Ph.D.)

Isolation, characterisation and mode of action of a new cardenolide cryptosin by R. Venkateswara.
Research supervisor: C. S. Vaidyanathan.
Department: Biochemistry.

1. Introduction

Coronary and hypertensive heart diseases constitute nearly 60% of the disease incidence of heart in industrialised countries. Cardiac failure is the most characteristic clinical symptom of most of these heart diseases.

Cardiac glycosides are the most useful drugs available for the treatment of cardiac failure. They

are of plant origin and their occurrence has been reported in a number of plant families. Particularly, *Asclepiadaceae* and *Apocynaceae* families are rich sources of cardenolides[1]. *Asclepiadaceae* members, commonly known as milkweeds, are popular in folk medicine. Phytochemically they are a source of cardio-active and cytotoxic glycosides. Although a number of reports have indicated the occurrence of cardio-active glycosides in the *Asclepiadaceae* family, a detailed investigation on a milkweed has not yet been attempted. We, therefore, undertook an extensive study on Indian milkweed *Cryptolepis buchanani* Roem & Schult.

2. Experimental and discussion

Acetone extract of the leaves gave positive tests for the presence of cardenolides. Further processing resulted in the isolation of a crystalline glycoside, hitherto unreported, to which we coined the name 'Cryptosin' after its source. By means of different chemical and spectroscopic methods we elucidated the chemical structure of cryptosin. Single crystal structure was solved by employing X-ray analysis.

Cryptosin was found to have certain unique structural features such as the presence of a C-11 β-oriented hydroxyl, C-12 carbonyl oxygen and C-7, C-8 α-epoxide. Further, the glycone was a 2-deoxyglucose attached at C-3 position. Since the structural features were characteristic of a cardiac glycoside, we subjected cryptosin to a pharmacological screening.

The positive inotropic effect of cryptosin was evaluated on spontaneously beating guinea pig right atrial preparations and dog heart was used for *ex vivo* studies. Pharmacologically, cryptosin was found to be a positive inotropic agent and the effect was dose-dependent. The maximum inotropic effect produced by cryptosin was about 25% less than that produced by ouabain. The ED-50 for cryptosin was calculated to be 1 μM which is about two fold higher than that of ouabain. Interestingly, cryptosin produced a positive chronotropic effect. A 23% increase in the rate above the basal level was observed at a dose of 1 μM.

Our interest was to understand the biochemical mode of action of cryptosin. Since cardiac glycosides are believed to produce positive inotropic effect *via* the inhibition of the Na, K-ATPase, the interaction of cryptosin with Na, K-ATPase was investigated[2].

Different sources of Na, K-ATPase enzyme including dog heart, guinea pig heart and highly purified enzyme (Sigma) were used. Cryptosin inhibited the Na, K-ATPase enzyme obtained from all the three sources, and as expected the extent of inhibition was dependent on the source of enzyme. The degree of inhibition of the enzyme from a particular source, in the presence of cryptosin, is varied with the concentration of cryptosin until a pleateu is reached. Corresponding to the pleatuing concentration of cryptosin a maximum inhibition of up to 85% of the original enzymatic activity was observed. Dixon-plot analysis of the inhibition of ATP hydrolysis by cryptosin yielded a K_i value of 32 μM as against 39 μM for ouabain. A novel 32P NMR spectroscopic method to monitor ATP hydrolysis by Na, K-ATPase in the presence and absence of cryptosin was employed. Both conventional and 32P NMR spectroscopic methods gave consistent results. It was interesting to note that cryptosin had comparable inhibitory potency with ouabain on Na, K-ATPase.

Recent suggestions that Na, K-ATPase is the 'receptor enzyme' for the cardiac glycosides prompted us to study the interactions of cryptosin with cardiac glycoside-binding sites[3]. Since 3H-cryptosin was not available, we used 3H-ouabain as the binding radioligand. Guinea pig heart membrane preparations were used for *in vitro* filtration binding assays. Ouabain binding as a function of exogeneous cryptosin showed a 84% inhibition of the labelled ouabain binding at a concentration of 100 μM cryptosin. A 50% displacement concentration for cryptosin was found to be 1 μM for ouabain-binding sites. The physiological response in guinea pig atrial preparations and dog heart

was in the range of 0.1 to 10 μM with a maximum response at 100 μM corroborated well with the results of binding study.

Cardiac calcium-channel blockers block the entry of extracellular calcium and thus antagonise the positive inotropic effect of cardiac glycosides[4]. Further, the nature of interdependence of Na, K-ATPase and calcium channels is unknown. We therefore set forth a study on the effects of cryptosin on dihydropyridine type of calcium channels. We quantitated the dihydropyridine type of calcium channels using 3H-PN200-110 as the radioligand. Cryptosin pretreatment of the membrane altered the calcium channel density specific of PN200-110. A 44 and 66% decrease in the densities was observed in guinea pig and dog heart membranes, respectively. The apparent dissociation constant (K) for PN200-110 to its binding sites was not altered significantly due to the presence of cryptosin.

Although by no means complete, we suggest that cryptosin in particular and cardiac glycosides in general may indirectly influence calcium channels *via* the alteration of the recycling frequency of Na, K-ATPase, as a sequel to which the mobility of calcium across the membrane is altered.

3. Conclusion

In summary, a new cardenolide was isolated, structure elucidated and its effect on mammalian heart was studied. Further, the biochemical mode of action was investigated.

References

1. HASHIMOTO, T., RATHORE, H., SATOH, D., HONG, G., GRIFFIN, J. F., FROM, A. H. L., AHMED, K. AND FULLERTON, D. S. — *J. Med. Chem.*, 1986, **29**, 997-1003.
2. AKERA, T. — *Science*, 1977, **198**, 569-574.
3. LANGER, G. A. — *Fed. Proc.*, 1977, **36**, 2231-2234.
4. HEIREM, E. AND NOACK, E. — *Arch. Expl Path. Pharmac.*, 1972, **275**, 359-371.

Thesis Abstract (Ph.D.)

Microbial degradation of the herbicide, 2, 4-dichlorophenoxyacetic acid: Studies on 2, 4-dichlorophenol hydroxylase in *Pseudomonas cepacia* by V. Radjendirane.
Research supervisor: C. S. Vaidyanathan.
Department: Biochemistry.

1. Introduction

Among the groups of chlorinated aromatic hydrocarbons, 2, 4-dichlorophenoxyacetic acid (2, 4-D) and related chlorophenoxy-alkanoic acids have become substantial environmental pollutants because of their world-wide employment as herbicides against broad-leaved plants, since the early 1940s. Microorganisms remarkably adapt themselves to these recalcitrant compounds and degrade them by enzymatic hydroxylation thereby increasing their solubility in the aqueous environment, decreasing their toxicity and rendering them susceptible to further degradation. The aim and scope of this investigation was to isolate an organism which degrades the herbicide, 2, 4-D and to demonstrate the pathway for its degradation in the isolated organism, *viz.*, *Pseudomonas cepacia* and to study the

enzymes involved in the degradation, namely, 2,4-D monooxygenase, 2,4-dichlorophenol (DCP) hydroxylase and 3,5-dichlorocatechol dioxygenase. 2,4-Dichlorophenol hydroxylase was chosen for a detailed study in view of its importance as one of the flavoprotein monooxygenases, a group of enzymes involved in the detoxification of toxic environmental pollutants.

2. Results and discussion

2.1. *Isolation and characterization of a bacterium that degrades 2,4-dichlorophenoxyacetic acid*

2,4-Dichlorophenoxyacetic acid-degrading bacterial strain, *Pseudomonas cepacia* was isolated from soil contaminated with an industrial effluent from 2,4-D manufacturing industry, by enrichment culture technique (Fig. 1).

2.2. *Metabolism of 2,4-dichlorophenoxy acetic acid by Pseudomonas cepacia*

This organism utilizes 2,4-D as sole source of carbon and energy in basal salt liquid medium up to relatively high concentration of 0.25%. We observed nearly quantitative conversion of the organically bound chlorine in 2,4-D to the inorganic form and so concluded that the molecule suffered complete decomposition and this was also supported by the 2,4-D depletion monitored by HPLC.

The intermediates of the pathway, namely, 2,4-dichlorophenol and 3,5-dichlorocatechol were isolated from the spent medium and identified by GC, HPLC and GCMS. Thus a pathway was proposed for the degradation of 2,4-D, namely, 2,4-D → 2,4-dichlorophenol → 3,5-dichlorocatechol → 2,5-dichloromuconic acid.

2.3. *Purification and properties of 2,4-dichlorophenol hydroxylase*

The enzyme 2,4-dichlorophenol hydroxylase was purified by affinity chromatography. The affinity column was prepared by coupling 2,4-dichlorophenol with epoxy-activated Sepharose 4B-CL (Fig. 2). The enzyme was desorbed from the matrix in the presence of substrate 2,4-dichlorophenol. The homogeneity of the enzyme was established by PAGE, both under non-denaturing and denaturing conditions, immunoelectrophoresis and analytical ultra centrifugation. The enzyme had a molecular

FIG. 1. The transmission electron micrograph of *Pseudomonas cepacia*.

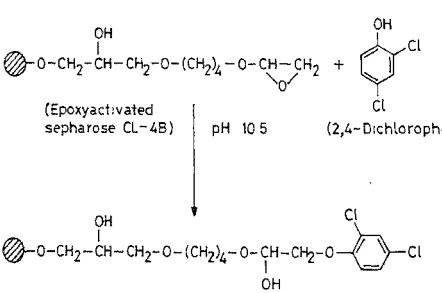

FIG. 2. Preparation of 2,4-dichlorophenol coupled to epoxy-activated Sepharose CL-4B.

weight of 275.000 as determined by gel permeation on a calibrated superose™ 6 column. SDS-PAGE showed a single band with a molecular weight of approximately 67,000 suggesting the native enzyme to be a tetramer of identical subunits. The enzyme required NADPH, FAD and molecular oxygen for activity. The product of the enzyme reaction was identified as 3, 5-dichlorocatechol based on GC, HPLC and GCMS studies.

The K_m for the aromatic substrate, 2, 4-DCP, determined from the rate of: (*i*) consumption of oxygen, and (ii) disappearance of NADPH, were 14 and 19 μM, respectively. The enzyme had a preference for NADPH to NADH. The K_m for FAD was obtained by reconstitution of apoprotein with FAD which was found to be 73 nM. Atebrin, a competitive inhibitor of flavoprotein monoxygenases, caused considerable inhibition of the enzyme activity.

The variance of log K_m of 2, 4-DCP as function of pH was plotted. From this plot, pK_a value for the ionisable group involved in catalysis was calculated to be 7.2, which corresponds to the pK_a value of histidine and/or cysteine. Free histidine has a pK_a of 6.5 and in proteins the value ranges from 5.5 to 7.5.

Several analogs of 2, 4-DCP inhibited 2, 4-DCP hydroxylase. Potent inhibition was observed in the case of 2, 4, 5-trichlorophenol ($K_i = 54\ \mu M$) and 2, 4, 6-trinitrophenol ($K_i = 82\ \mu M$). Both the compounds inhibited the enzyme in a competitive manner[1].

The absorption spectrum of 2, 4-DCP hydroxylase was characteristic of a flavoprotein with a major peak at 278 nm and two other peaks in the visible region at 370 and 452 nm.

The fluorescence emission properties of the enzyme were characteristic of a protein containing tryptophan residues. The enzyme had excitation and emission maxima at 284 and 328 nm, respectively.

The circular dichroism (CD) spectrum of 2, 4-DCP hydroxylase in the far-UV (200–250 nm) region showed that the enzyme had a significant amount of α-helical secondary structure.

2.4. *Studies on the active-site amino-acid residue of 2,4-dichloro phenol hydroxylase*

The enzyme 2,4-DCP hydroxylase was probed for the active-site amino-acid residues using modification reagents specific for arginine, histidine and tryptophan. Arginine residues in the enzyme were modified using phenylglyoxal. From the first order plots and double log-replot, the number of phenylglyoxal molecules required for complete inactivation was calculated to be 2.2 which suggested the occurrence of at least one arginine residue per active site. The inactivation by phenylglyoxal could be reversed by extensive dialysis against 50 mM phosphate buffer, pH 7.0, thereby showing that the loss of activity was due to the modification of arginine residue at the active site of the enzyme. The complete protection offered by NADPH implicated that the arginine residue was located at or near the NADPH-binding site of 2, 4-dichlorophenol hydroxylase. The guanidinium group of the arginine residue may interact with 2′-phosphate of NADPH electrostatically.

Histidine residues in the enzyme were modified using diethylpyrocarbonate (DEPC). From the first-order plots and from double log-replot the number of DEPC molecules required to inactivate one active center was calculated to be 1.0 suggesting at least one histidine residue per active site. The protection offered by 2,4-DCP suggested the presence of a histidine residue at or near the 2,4-DCP-binding site of the enzyme. The modified inactive enzyme was reactivated to 78% by treatment with hydroxylamine suggesting that the amino acid modified was a histidine residue. This was further confirmed by the difference spectrum of the DEPC-treated enzyme which showed a peak at 247 nm due to the formation of carbethoxy derivative of histidine. Histidine residue is probably involved in hydrogen bonding with hydroxyl group of the substrate.

Tryptophan residues were modified using N-bromosuccinimide. The modification experiments revealed the involvement of one tryptophan residue per active site of the enzyme. This was further supported by the protection offered by the substrate 2,4-dichlorophenol. It might be conjectured that tryptophan forms a charge-transfer complex with the aromatic ring of 2,4-dichlorophenol.

2.5. *Studies on the interaction of 2,4-dichlorophenol with 2,4-dichlorophenol hydroxylase*

Binding of the substrate, 2,4-DCP, to the enzyme caused a marked perturbation in the visible absorption spectrum of the enzyme, suggesting the formation of an E–S complex. The geometric proximity of tryptophan and arginine at the active site probably accounts for the perturbations of the fluorescene emission spectrum of the active-site tryptophan of the flavoenzyme. The change in the near UV-CD spectrum of the flavoenzyme under conditions when the active-site arginine was selectively modified by phenylglyoxal further supports the proposal of geometric proximity of the active-site tryptophan and the arginine. The presence of a potential chromophoric group such as phenyl group perturbs the chiral environment of the tryptophan residues, hence the alteration in the side-chain CD spectrum.

The probable involvement of arginine in E–S complex formation is indicated by the comparative affinities of the E–S complex for the unmodified and the modified enzyme. The decrease in the affinity constant probably occurs as a sequel to the absence of non-covalent stabilization interaction such as electrostatic or hydrogen bonding. The present results clearly indicate the role of arginine in the E–S complex formation.

The reduced affinity constants of the DEPC-modified enzyme for the substrate suggest the involvement of the histidine residues in the E–S complex formation *via* potential hydrogen bonding loci of the imidazole group of histidine and the hydroxyl group of the substrate.

NBS-induced quenching of the protein fluorescence and observed decrease in CD band in the near-UV region of the NBS-modified enzyme shows clearly the presence of tryptophan at the active site. The observed decrease in affinity constant of the NBS-modified enzyme and the substrate probably suggest that its aromatic ring stabilizes the E–S complex *via* charge-transfer interaction with the substrate.

Tryptophan, arginine and histidine are the amino acids involved in the binding of the substance to the flavoenzyme. The tryptophan residue imparts stability to the complex probably *via* charge-transfer interaction with the aromatic ring of the substrate; histidine is probably involved in H-bonding interaction with the potential donor (Cl) or acceptor (–OH) sites of the substrate.

2.6. *Studies on the interaction of FAD with 2,4-dichlorophenol hydroxylase*

Flavin moiety was successfully removed from the native flavoenzyme to get an apoprotein[2]. The reconstitution of the apoprotein and the flavin to form an active flavoenzyme supports a non-covalent nature of interaction. Absence of any significant changes in the far UV-CD spectrum upon addition of flavin to the apoprotein clearly indicates that there is no change in the α-helical content of the apoprotein due to the addition of flavin. This was further supported from a comparison of the CD spectra of the native flavoprotein and apoprotein.

The reduced slope for the straight line corresponding to the quenching of the flavoprotein fluorescence by acrylamide indicates that the tryptophan residue becomes less accessible. There is a blue shift of the 278 nm peak of the apoprotein to 273nm upon addition of flavin to the apoprotein. All these features suggest interaction between the isoallaxazine ring of FAD and the aromatic side chain such as tryptophan of the flavoenzyme.

The progressive increase in the FAD fluorescence upon addition of NBS favours interaction between the isoalloxazine ring and the tryptophan residue which gets specifically modified in the presence of NBS. The extent of charge-transfer interaction between the FAD and the modified tryptophan with reduced aromaticity decreases, thereby leading to de-quenching of the flavin fluorescence.

The comparison of the side-chain CD spectra of the flavoenzyme and the apoenzyme also favours an interaction involving the aromatic amino-acid residues of the protein and the flavin in the flavoenzyme. The presence of a positive and negative maxima in the 280–310 nm region probably arises out of the coupling (Davydov type) of the alloxazine chromophore in FAD and the tryptophan residue(s) of the protein.

3. Conclusion

In conclusion, the results presented show that the herbicide 2,4-D is metabolized *via* 2,4-dichlorophenol and 3,5-dichlorocatechol in *Pseudomonas cepacia*. A flavoprotein, 2,4-DCP hydroxylase, induced by 2,4-D catalyses the *ortho* hydroxylation of 2,4-DCP to 3,5-dichlorocatechol with the consumption of NADPH and molecular oxygen. The enzyme 2,4-DCP hydroxylase was purified to homogeneity by affinity chromatography. As a preliminary step to understand the chemistry of action of this enzyme, we undertook a detailed physico-chemical investigation of the reversible complex (i) between the oxidised flavoenzyme and the substrate, and (ii) between the apoprotein and FAD. The chemical modification and the physico-chemical investigations revealed the probable involvement of arginine and histidine at the 2,4-DCP-binding site and of tryptophan at the FAD-binding site.

References

1. DIXON, M. *Biochem. J.*, 1953, **55**, 170–172.

2. MASSEY, V. AND CURTI, B. *J. Biol. Chem.*, 1966, **241**, 3417–3423.

Thesis Abstract (Ph.D.)

Involvement of lipid peroxidation in thermogenesis: Mediation by alpha-adrenergic receptor under cold stress and noradrenaline treatment by B. Seshadri Sekhar.
Research supervisors: T. Ramasarma and C. K. Ramakrishna Kurup.
Department: Biochemisty.

1. Introduction

Increases in basal metabolic rate and oxygen consumption occur on chronic exposure of animals to cold temperatures. This process which follows shivering thermogenesis is known as regulatory 'non-shivering thermogenesis'. A variety of explanations such as uncoupling of oxidative phosphorylation, futile cycles involving wasteful turnover of ATP interlocking a phosphatase and a kinase, shunt pathways of electron transfer to bypass ATP-coupling sites, and uncoupling of proton gradient from ATP synthesis, have been offered to account for non-shivering thermogenesis[1,2]. Thermogenin (uncoupling protein)-mediated discharge of proton gradient proposed for brown adipose tissue (BAT) may not be applicable to other tissues[3]. Moreover, the uncoupling protein is not known to be regulated by physiological modulators like hormones. An effort was made in the present investigation

to look at the involvement of mitochondrial H_2O_2 generation and microsomal lipid peroxidation in the mediation of non-shivering thermogenesis.

2. Materials and methods

Male albino rats of the Wistar strain were exposed to cold (0–4°C) or heat (38 ± 1°C) for four weeks. Control animals were kept at 24 ± 1°C. Mitochondria and microsomes were isolated from liver and BAT by differential centrifugation. Mitochondrial H_2O_2 generation[4] and microsomal lipid peroxidation[5] were measured. Cytochrome content was computed from difference spectra. The activity of NAD(P)H-cytochrome *c* reductase was measured by spectrometry. Lipid peroxidation was measured by O_2 uptake and malondialdehyde (MDA) formation.

3. Results and conclusions

This is the first report on the generation of H_2O_2 by BAT mitochondria. Succinate, glycerol-1-phosphate and fatty acyl CoA were good substrates for the reaction while NAD^+-linked substrates were less effective. The rate of H_2O_2 generation by BAT mitochondria was almost five times as high as that by hepatic mitochondira. Upon cold-acclimation of rats, the rate of H_2O_2 generation by BAT mitochondria increased two fold. This is consistent with the thermogenic role assigned to the tissue and the reaction. In effect, due to the large increase (5–6 fold) in the size of the tissue, the rate of generation of H_2O_2 increased more than ten fold on cold exposure. The respiratory activity of BAT

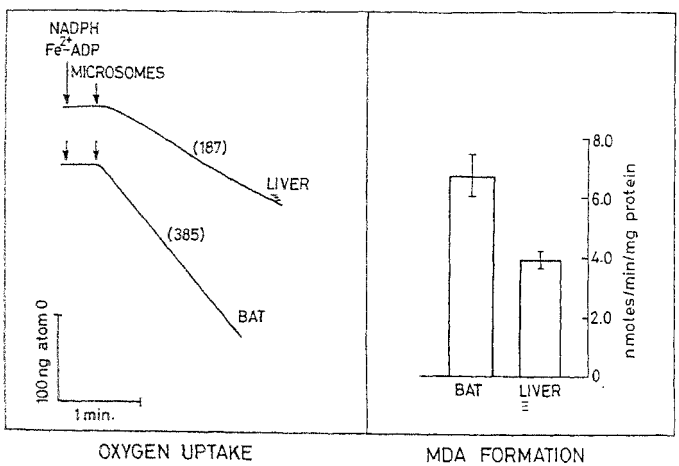

FIG 1. Lipid peroxidation in liver and BAT microsomes of cold-acclimated animals. Rats were exposed to cold (0–5°C) for 30 days. Microsomal lipid peroxidation was measured both by oxygen uptake and malondialdehyde (MDA) formation. The value in parenthesis represents atom O taken up/min/mg protein.

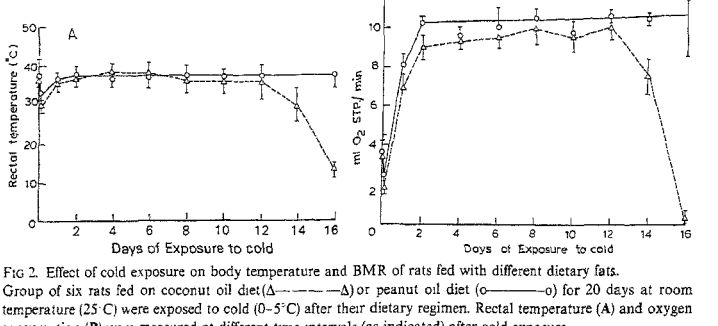

FIG 2. Effect of cold exposure on body temperature and BMR of rats fed with different dietary fats. Group of six rats fed on coconut oil diet(Δ———Δ) or peanut oil diet (o———o) for 20 days at room temperature (25°C) were exposed to cold (0–5°C) after their dietary regimen. Rectal temperature (**A**) and oxygen consumption (**B**) were measured at different time intervals (as indicated) after cold exposure.

mitochondria did not increase on cold exposure. These positive findings notwithstanding, H_2O_2 generation by itself accounts for only 2% of the total O_2 consumption and, therefore, cannot account for non-shivering thermogenesis.

Microsomal lipid peroxidation which entails rapid oxygen uptake and NADPH oxidation has been recognized as an energy-dissipating reaction[5]. Consistent with this, microsomal lipid peroxidation in both liver and BAT increased upon exposure of animals to cold stress by about three fold. In cold-exposed rats, the rate of microsomal lipid peroxidation was higher in BAT than in liver (Fig. 1).

Interestingly enough, BAT was found to be devoid of cytochrome P_{450}. Moreover, the rate of biosynthesis of isoprenoid compounds was low in the tissue, although the concentrations of cholesterol and ubiquinone were high.

Non-shivering thermogenesis is known to be regulated by the α-adrenergic-receptor system[1]. Consistent with this, it was found that noradrenaline could induce lipid peroxidation in rat hepatic microsomes. Hormone-mediated induction was effectively blocked by antagonists of adrenergic, but not by β-adrenergic, receptors.

Since polyunsaturated fatty acids are the substrates for lipid peroxidation, the role of dietary unsaturated fatty acids in cold acclimation was investigated. Rats fed with dietary fat rich in saturated fatty acids could not survive for more than 16 days when exposed to cold (0–5°C) temperatres. Their body temperature and oxygen consumption decreased dramatically at this time interval. Animals fed with unsaturated fat did not show any adverse effect when exposed to cold (Fig. 2). This experiment illustrated the importance of dietary fatty acids in adaptation to cold temperature.

References

1. JANSKY, L. Nonshivering thermogenesis and its thermoregulatory significance, *Biol. Rev.*, 1973, **48**, 85–132.

2. RAMASARMA, T. AND SIVARAMAKRISHNAN, S. Effect of environmental stress of cold and hypobaria on coenzyme Q metabolism and Q-dependent reactions; in *Biomedical and clinical aspects of coenzyme Q* (Folkers, K. and Yamamura, Y., eds), 1977, pp 131–150, Elsevier.

3. RAMASARMA, T., SEKHAR, B. S. AND KUPLR, C. K. R.	Cellular thermogenesis: a new approach; in *Bioenergetics: Structure and function of energy transducing systems* (Ozawa, T. and Papa, S., eds), 1987, pp 225–233, Japan Sci. Soc. Press, Tokyo.
4. SEKHAR, B. S., KURUP, C. K. R. AND RAMASARMA, T.	Generation of hydrogen peroxide by brown adipose tissue mitochondria, *J. Bioenergetics Biomembranes*, 1987, **19**, 397–407.
5. RAMASARMA, T., KELLY, M. S AND HOCHSTEIN, P	Inhibition of microsomal lipid peroxidation by cytosolic protein in presence of ADP and high concentrations of Fe^{2+}. *Biochim. Biophys. Acta*, 1984, **796**, 243–250.

Thesis Abstract (Ph.D.)

Transcription of rDNA in rice by K. Nandabalan.
Research supervisor: J. D. Padayatty.
Department: Biochemistry.

1. Introduction

The genes for the rRNAs in plants, like in all other eukaryotes, are organized in tandemly repeated arrays, and are highly reiterated. The ribosomal DNA (rDNA) is transcribed as a single unit yielding a 35–47 S precursor which is processed to give the mature 25–28, 17–18, and 5.8 S rRNAs. Though much information is available now on the regulation of rDNA expression in animals, not much progress has been made in plants. With a view to understand this, rDNA unit from rice embryos was isolated, and the rRNA genes and the sites for the transcription initiation and termination were mapped.

2. Experimental and discussion

A clone bearing a 9.8-kb insert DNA containing the rDNA unit of rice was identified by screening an *Eco*RI genomic library of rice DNA in Lambda Charon 4 phage with ^{32}P-18 S rRNA[1]. The organization of the 18, 5.8 and 25 S rRNAs on this rDNA was determined by the hybridization of ^{32}P-end-labelled rRNAs to the *Bam*HI fragments of the 9.8-kb DNA and confirmed by partially sequencing the individual rRNA genes. The partial sequences of the 18, 5.8 and 25 S rRNA genes of the rice variety IR-20 were identical to those in the rice variety Magnetsumochi[2]. The genes for the rRNA are present in the order 18–5.8–25 S.

The intergenic spacer (IGS) between the 18 and 25 S rRNA genes was sequenced, and a sequence of 1482 nucleotides upstream to the 18 S rRNA gene, and a sequence of 849 nucleotides downstream to the 25 S rRNA gene were obtained[3]. The region of the IGS upstream to the 18 S rRNA gene is characterized by the presence of three long direct repeats, the first of which starts from the 526th nucleotide upstream to the 18 S rRNA gene. The first repeat is 320 nucleotides long, and the third repeat which is 238 nucleotides long appears to be a truncated one.

The M13mp18 clone bearing the DNA spanning the region of the IGS immediately upstream to the 18 S rRNA gene was hybridized simultaneously to the 5′-end-labelled 15-mer universal primer and the nuclear RNA isolated from rice embryos. The primer was extended with reverse transcriptase and the size of the extended product was determined on a sequencing gel. From such a primer extension analysis the site for the initiation of transcription was found within the first repeat, at an A, 623 nucleotides upstream to the 18 S rRNA gene. Different stretches of DNA spanning the entire IGS were fused to the chloramphenicol acetyl transferase (CAT) structural gene and were transcribed in

intact nuclei isolated from rice embryos. The CAT-specific transcripts were detected by S1 nuclease mapping using ^{32}P-labelled CAT structural gene as the probe. All the rDNA-CAT constructs yielded CAT-specific transcripts in the presence of α-amanitin, indicating the presence of multiple promoters for rDNA transcription. However, the extent of protection from S1 nuclease digestion was more when the promoter nearest to the 18 S rRNA gene was used, than the upstream promoters. This indicated that the upstream promoters present are weaker than the one next to the 18 S rRNA gene.

The sequence of 849 nucleotides of the IGS downstream to the 25 S rRNA gene is characterized by the presence of two repeats which are 204 and 212 nucleotides long. The last 98 nucleotides of the sequence obtained in this region seem to be a part of the third repeat. These repeats are not homologous to the repeats present upstream to the 18 S rRNA gene.

The 3′-^{32}P-end-labelled DNA fragments spanning the IGS downstream to the 25 S rRNA were hybridized to nuclear RNA, digested with S1 nuclease and the size of the resulting hybrids was determined. From the sizes of the protected DNA fragments, two 3′ termini of transcription were derived and found to be at 616 and 620 nucleotides downstream to the end of the 25 S rRNA gene[4]. This is different from that of in maize and radish where the termination sites coincide with the end of the 25 S-rRNA gene. The 18-nucleotide motifs at the termination sites in rice and mouse rDNAs are homologous, albeit in the reverse orientation[5].

References

1 NANDABALAN, K. AND PADAYATTY, J. D. *Indian J Biochem. Biophys.*, 1989, **26**, 289–292.

2. TAKAIWA, F., OONO, K., IIDA, Y. AND SUGUIRA M. *Gene 37*, 1985, 255–259.

3. NANDABALAN, K. AND PADAYATTY, J. D. *Biochem. Biophys. Res. Commun.*, 1989, **160**, 1117–1123.

4. NANDABALAN, K. AND PADAYATTY, J. D. *Biochem. Biophys. Res. Commun.*, 1988, **157**, 68–74.

5 GRUMMT, I., ROSENBAUER, H., NEIDERMEYER, I., MAIER, U. AND OHRLEIN, A. *Cell*, 1986, **45**, 837–846.

Thesis Abstract (Ph.D.)

Purification and characterization of DNA cytosine 5-methyltransferase in a mealybug *Planococcus lilacinus* and studies on its modulation during development by C. Devajyothi.
Research supervisor: H. Sharat Chandra.
Department: Microbiology and Cell Biology.

1. Introduction

DNA methylation is the most widely known form of DNA modification. In most higher organisms, DNA is modified after synthesis by the enzymatic conversion of cytosine into 5-methylcytosine. This methylation is carried out by a DNA methyltransferase using S-adenosyl methionine as a specific methyl group donor. In many systems, undermethylation of certain DNA sequences is correlated

with gene expression[1]. Evidence suggesting a relationship between methylation and X-chromosome inactivation has been obtained in cells of mammalian females[2]. A system of facultative inactivation of whole chromosome—similar to that of the mammalian X-chromosome—also occurs in mealybugs and related coccid insects. These insects therefore appear to offer an attractive model system for studying the relationship between chromosome inactivation, DNA methylation and certain developmental events. We have chosen for this investigation *Planococcus lilacinus* [Coccoidea, Homoptera], a sexually reproducing mealybug. Both males and females of this insect start development with ten chromosomes, but during early embryonic development the paternally derived set of chromosomes become heterochromatic in most tissues of those embryos that develop into males. In females, both sets of chromosomes remain euchromatic and genetically functional. Sex appears to be determined by the presence of one or two active sets of chromosomes. Methylation of DNA is thought to be one of the factors determining differential regulation of homologous chromosomes within the same nucleus[3]. The mealybug system thus seems to offer a better opportunity than mammalian X-chromosome for studying the role of DNA methylation in chromosome inactivation because 50% of the genome is inactive in most of male mealybug nuclei, whereas the inactive-X comprises only 7% of the genome in female mammals. In mealybugs, chromosome inactivation is sex-determining, and a hypothesis suggests that in mammals, too, this inactivation may be sex-determining[4,5]. The role of cytosine methylation is well documented in gene regulation, but its role, if any, in inactivation of entire chromosomes is not understood. It was therefore felt that purification and characterization of DNA methyltransferase from *P. lilacinus* and a study of its sequence specificity and developmental regulation might provide useful clues about the unusual genetic system of mealybugs.

2. Experimental approach

The study involved the purification of enzyme through several ion exchange and molecular sieve columns. As a final step in purification affinity chromatography on SAH-agarose column was used. The assays for monitoring the activity were carried out using radioactive methyl donor, namely, S-adenosyl-$^{14}CH_3$-methionine[6].

3. Results and discussion

A cytosine-specific DNA methyltransferase [E.C.2.1.1.37] has been purified to homogeneity from *P. lilacinus* by DEAE-cellulose, hydroxyapatite and SAH-agarose chromatography. The enzyme appeared as a single band on 7.5% PAGE and as two bands of M, 65,000 and 60,000 on 7.5% SDS-PAGE. When the enzyme was passed through Superose-6 gel filtration column on FPLC, it showed three peaks but the activity was seen only in the fractions corresponding to the first peak. Molecular weight of this peak corresponds to that of a marker protein, alkaline phosphatase [M, 1,40,000]. The enzyme has been characterized in terms of its affinity for DNA and S-adenosyl methionine, optimum pH, requirement for EDTA, salt and sulfydryl compounds. The effect of various inhibitors on the enzyme was also studied.

The availability of a homogenous preparation of methyltransferase made it possible to study its substrate and sequence specificity and its mode of action. The mealybug enzyme methylated both native and denatured DNAs but it preferred denatured DNA. Enzyme activity was not found to be proportional to GC content in DNA which may be due to methylation of cytosines in dinucleotides other than CpG. *de novo* DNA methyltransferase activity was determined by using various synthetic polymers. Among the synthetic polymers tested, poly[dI–dC]. poly[dI–dC] was a better substrate than poly[dG–dC]. poly[dG–dC]. The enzyme requires alternating cytosine-purine residues in polydeoxyribonucleotides for the transmethylation reaction to occur. Poly[dI–dC]. poly[dI–dC]

does not represent a naturally occurring dinucleotide, but some unknown conformational feature renders this polymer a better substrate. No difference in methylation levels was observed when assays were done with undigested phase and SV40 DNAs compared with the same DNAs digested with *Hpa* II and S_1 nuclease. This indicated that sequences other than OCGG are recognised by the mealing enzyme. RNA inhibits enzyme activity, suggesting possible *in vivo* regulation of the enzyme by RNA.

Studies of temperature-dependent effects of salt on enzyme activity suggests that the formation of a tight, salt-resistant complex is necessary for DNA methylation to occur. A processive mode of action has been postulated on the basis of dual-substrate reactions where once the enzyme is bound to DNA, the later addition of any substrate does not cause a change in the amount of methylation.

If methylation is related to imprinting and heterochromatization of mealybug chromosomes, any sex-specific differences in methylation should be reflected in the sequence specificity and the levels of DNA methyltransferase(s) in the two sexes during different stages of development. A partially purified enzyme from different instars was used in a comparative study. The enzyme from second instar females did not show any activity with any of the substrates whereas the enzyme from the third instar females showed a high level of methyl group incorporation which is maintained at that level in fourth instar also. Reciprocal assays were also carried out using the enzyme from female mealybugs and male DNA in one set and the enzyme from male mealybugs with female DNA in another set. The male enzyme was able to methylate female DNA but the reverse did not occur. This suggests that the sites of methylation in the two sexes might be different. Also no homologous methylation (that is, male enzyme with male DNA and female enzyme with female DNA) was detectable which suggests that all the internal sites are methylated and that unmethylated sites may not have been available for methylation by the homologous enzyme. If the sites of DNA methylation in male and female mealybugs differ in sequence, it should be possible to detect these differences using synthetic polynucleotides. The activity with CpA-, CpI- and CpG-containing polymers which is totally absent in second instar females reaches a peak in third instar, and is maintained at that level in fourth instar females also. The enzyme from adult males and gravid females is not able to methylate CpA as efficiently as the enzyme isolated from other stages. During the methylation of third and fourth instars of development, methylation of cytosines in the dinucleotides CpA and CpI was higher than that in CpG.

It is possible to correlate the above results with mealybug development. There are five instars distinguishable in males, and four in females. The two sexes can be distinguished morphologically from the second instar onwards. Gametogenesis starts at the third instar in both the sexes and fertilization occurs during the fourth instar. Inactivation of the paternal set of chromosomes in male embryos is known to occur during early stages of mealybug development. If DNA methylation is implicated in inactivation of chromosomes, significant levels of *de novo* methylation should occur at these stages. However, males are expected to contain high levels of maintenance methylase throughout development. The appearance of high levels of *de novo* methyltransferase(s) in the third and fourth instar females may be to ensure that the paternal set of chromosomes are imprinted and inactivated. Thus our results are consistent with the view that one component of the control of chromosome inactivation may be modulation of the levels of DNA methyltransferase(s) during mealybug development[6].

References

1. DOERFLER, W — *A. Rev. Biochem.*, 1983, **52**, 93–124.

2. RIGGS, A. D. — *Cytogenet. Cell Genet.*, 1975, **14**, 9–25.

3. HOLLIDAY, R. AND PUGH, J. E. *Science*, 1975, **187**, 226–232.

4. CHANDRA, H. S. PNAS, 1985, **82**, 6947–6949.

5. SIMON, D., GRUNERT, F., ACKEN, U., DORING, H. P. AND KROGER, W. *Nucl. Acids Res.*, 1978, **5**, 2153–2167.

6. DEVAJYOTHI, C. AND BRAHMACHARI, V. *FEBS Lett.*, 1989, **250**, 134–138.

Thesis Abstract (Ph.D.)

Effect of nucleic-acid-reactive antibodies on transformed cells grown *in vitro* by Y. N. Vaishnav.

Research supervisors: A. Antony and G. Ramananda Rao.
Department: Microbiology and Cell Biology.

1. Introduction

Nucleic-acid-reactive antibodies have been extensively used in various biochemical investigations[1,2]. These antibodies have been shown to inhibit some of the nucleic-acid functions in cell-free systems. High rate of endocytosis has been reported in many types of transformed cells in contrast to most of the normal cells. Therefore, the use of nucleic-acid-reactive antibodies may offer a promising approach to selectively inhibit the growth of transformed cells. The present study was underaken to investigate (i) the effect of experimentally induced nucleic-acid-reactive antibodies on primary cell cultures and various established transformed cells, (ii) the mode of uptake and subcellular localization of the pinocytosed antibodies in transformed cells, and (iii) the potential of these antibodies to inhibit various nucleic-acid functions in cell-free systems.

2. Experimental

Adenosine was coupled to BSA by periodate oxidation method[3] and antibodies were raised in rabbits. IgG was obtained by sodium sulphate fractionation method and binding of antibodies to DNA and RNA was characterized by a highly sensitive avidin-biotin microELISA. Briefly, RNA DNAs were attached to poly-L-lysine-coated microtitre plates, serial dilutions of antiserum added and nucleic-acid-bound antibodies were detected by biotinylated goat anti-rabbit IgG in combination with HRP-avidin using H_2O_2 as substrate and *o*-phenylenediamine as chromogen. Fine specificity of anubody binding was further analysed using restriction fragments of DNA in gel retardation assay[4]. Antibodies were also raised against deoxydenylate (dpA), deoxycytidylate (dpC) and denatured DNA and binding of antibodies to dsDNA was characterized by avidin-biotin microELISA.

3. Results and discussion

Adenosine antibodies were found to inhibit the growth of various transformed cells in culture, *viz.*, HeLa, KB, HEp2, SP2/0 and Yoshida ascites sarcoma cells, as monitored by cell number and incorporation of radioactive precursors into DNA, RAN and protein. The inhibition was specific as antibodies after passing through adenosine-BSA-Sepharose did not inhibit cell growth. The inhibition

of cell growth due to the action of pinocytosed antibodies from within the cells was demonstrated by introducing adenosine antibodies into cytosol of HeLa cells by osmotic lysis of pinosomes which resulted in the inhibition of DNA, RNA and protein synthesis. The effect of antibodies on the distribution of cells in different phases of cell cycle, as studied by DNA flow cytometry, showed that cells in all phases of cell cycle were equally inhibited. The effect of adenosine antibodies on transformed cells appeared to be selective as they did not inhibit the synthesis of DNA, RNA and proteins in BALB c mouse lymphocytes. The fact that immunized rabbits remained apparently healthy even during hyperimmunization supported the view that the normal cells are probably not affected. Antibodies against dpA, dpC and denatured DNA did not inhibit the macromolecular synthesis in any of the cell lines studied.

Fluorescence microscopy studies revealed the uptake of antibodies and other proteins such as BSA by the transformed cells but not by lymphocytes. Non-specific nature of uptake, cytoplasmic granular fluorescence and the absence of binding of antibodies to cell surface indicated fluid-phase pinocytosis as the possible mode of uptake. This was confirmed by the kinetics of antibody uptake. Fluid-phase pinocytic activity of transformed cells was also shown by cytochemical demonstration and kinetics of uptake of HRP, a marker of fluid-phase pinocytosis. A highly sensitive cytochemical technique, using biotinylated secondary antibody and avidin-HRP, was employed to study subcellular distribution of pinocytosed antibodies. Adenosine antibodies were found accumulating in perinuclear region at 3 h of exposure. However, when chased for 24 h, antibodies could be seen diffused throughout the cytoplasm. Similar pattern was observed with anti-dpA, anti-dpC and anti-DNA antibodies, indicating that the inability of these antibodies to inhibit DNA, RNA and protein synthesis in transformed cells was not due to lack of uptake.

Having established that adenosine antibodies enter into the transformed cells and consequently inhibit cell growth, the effect of these antibodies and that of anti-dpA, anti-dpC and anti-denatured DNA on various nucleic-acid functions in cell-free systems was studied. Adenosine antibodies were found to inhibit *in vitro* transcription in isolated nuclei and with *E. coli* RNA polymerase. The inhibition was specific as it could be reversed by the homologous hapten. Various evidences indicated that the inhibition was due to the binding of antibodies to nascent RNA chains. The antibodies which react with DNA, but not with RNA such as anti-dpA, anti-dpC and anti-DNA, did not inhibit *in vitro* transcription in isolated nuclei or with *E. coli* RNA polymerase. The results clearly indicate that RNA-reactive population of adenosine antibodies is involved in the inhibition of transcription.

Anti-adenosine and anti-dpA, anti-dpC and anti-DNA antibodies did not inhibit *in vitro* DNA synthesis in isolated nuclei or with *E. coli* DNA polymerase I. Therefore, it appears that DNA-reactive antibodies, in spite of binding to DNA template, are not able to interfere with the process of transcription and DNA synthesis. However, RNA-binding population of adenosine antibodies may inhibit RNA primer formation at the initiation stage of *in vivo* DNA synthesis. Adenosine antibodies were also found to inhibit *in vitro* aminoacylation of tRNA and *in vitro* translation of endogenous mRNAs in rabbit reticulocyte lysate in a dose-dependent and hapten-specific manner. Antibodies against dpA, dpC and denatured DNA did not inhibit these processes. In conclusion, the present study has demonstrated that adenosine antibodies enter into transformed cells *via* fluid-phase pinocytosis and inhibit nucleic-acid functions leading to inhibition of growth of cells. The study also indicates the potential of RNA-reactive antibodies in the inhibition of nucleic-acid functions *in vitro* and *in vivo*.

References

1. STOLLAR, B. D. *Methods in enzymology*. Vol. 70, (eds) Vunakis, H. V. and Langone, J. J., 1980, pp 70–85, Academic Press.

2. STOLLAR, B. D. *CRC Crit. Rev. Biochem.*, 1986, **20**, 1–36.
3. ERLANGER, B. F. AND BEISER, S. M. *Proc. Natn. Acad. Sci. USA*, 1964, **52**, 68–74.
4. GARNER, M. M. AND REVZIN, K. *Nucleic Acids Res.*, 1981, **9**, 3047–3060.

Thesis Abstract (Ph.D.)

Regulation of fibroin H gene expression in the posterior silk glands of *Bombyx mori* by C. V. Patel.
Research supervisor: K. P. Gopinathan.
Department: Microbiology and Cell Biology.

1. Introduction

The larval silk glands of *B. mori* have long served as a model system for investigating developmentally regulated tissue and stage-specific gene expression[1]. The silk glands consist of a pair of long, tubular organs divided into anatomically and functionally distinct regions that produce the major classes of silk proteins. Fibroin, the silk fiber protein, is synthesized in posterior silk gland (PSG) and, sericin, the glue protein that coats the fibroin, is produced exclusively in middle silk gland (MSG).

The silk gland is fully formed at the end of embryonic development and no further cell division takes place. About 18–19 endomitotic replication cycles of DNA replication occur in the PSG and MSG in the larval stage. The cells in PSG and MSG become giant and during the last four days of the 5th instar, when the silk protein biosynthesis reaches maximal rates, 50% of the total protein produced by the larva is synthesized in the silk glands. This high level of silk protein synthesis has been a frequent topic of investigation. Fibroin H protein ($M_r \approx 350{,}000$) has an unusual amino-acid composition (Gly, 48%; Ala, 30%; Ser, 12%; Tyr, 4%) and is made up of several repetitive, identical peptide units[2]. The mRNA for fibroin H is also very long (15–16 kb) and is made up of short, identical, repetitive nucleotide sequences[3]. It is transcribed from a single copy gene and the transcription is regulated by a periodic 'turn-on and turn-off mechanism'[4]. The rate of fibroin H mRNA synthesis is determined to be 14 molecules/min/gene during the feeding stages of the 4th and 5th instar, while it drops by about 1000 fold during the moulting period.

There is a remarkable functional adaptation of the PSG in the final instar to synthesize high levels of fibroin H protein. As compared to the other genes, fibroin H gene is transcribed very efficiently in PSG cells and consequently enormous amounts of fibroin H mRNA accumulate. The translational machinery also adapts itself to the fibroin H synthesis. There is a dramatic increase in the levels of iso-accepting tRNAs for Gly, Ala, Ser and Tyr and their cognate synthetases so as to meet the demands for efficient translation of fibroin H-specific codons (Gly, Ala, Ser and Tyr[5]). Other species of poly $(A)^+$ RNAs and tRNAs undergo quantitative decrease. At the peak of fibroin H synthesis, 80% of the polysomes of giant PSG cells are engaged in fibroin H synthesis. Although the amount of fibroin H RNA as a per cent of total GSG RNA is identical during the feeding stages of the 4th and 5th instars, very little fibroin H protein is synthesized in 4th instar silk gland as compared to that produced in the 5th instar. Therefore, the transcriptional and translational regulation of fibroin H gene in the 4th and 5th instar (non-producing and producing stages of fibroin H, respectively) has been investigated.

2. The construction of genomic library of *B. mori*

Cloning of *B. mori* DNA was accomplished in the *Eco* RI site of Charon 4A bacteriophage vector. High efficiency *in vitro* packaging extracts were prepared and 2.8×10^5 recombinant-phage particles were obtained. A clone containing fibroin H sequence was isolated using ^{125}I labelled fibroin H RNA purified by Sepharose 4B chromatography and confirmed by RNase T_1 finger printing[6]. The clones were confirmed by positive hybridisation to the first cDNA strand synthesized from poly $(A)^+$ fibroin H mRNA. The insert size, orientation and putative map of the clone were obtained by restriction analysis.

3. Quantitation of fibroin H RNA, fibroin H protein, fibroin H mRNA and its polysome association in the 4th and 5th instar larval silk glands

The quantitation of fibroin H RNA was done based on gel exclusion HPLC and sucrose density gradient centrifugation analysis. The amount of fibroin H RNA as a percentage of total RNA was similar in feeding stages of the 4th and 5th instars, while it was rapidly degraded during the moulting stage. The percentage of polyadenylated fibroin H RNA in total fibroin H RNA obtained from the 4th and 5th instar larvae did not reveal any major difference. Anti-fibroin H antibodies were raised in rabbits and were purified, radioiodinated and used to quantitate (by filter-binding assay) fibroin H protein in the 4th and 5th instar silk glands. Compared to the 4th instar, fibroin H content was 17 fold higher in the 5th instar silk glands. The polysome association of fibroin H mRNA was checked to determine its translational ability. Poly $(A)^+$ RNA was obtained from the fibroin H polysomes (18,000 × g pellet), total polysome (80,000 × g pellet) and post-polysomal fraction of PSG from the 4th and 5th instars. When probed with end-labeled fibroin H DNA, only 40% of the fibroin H mRNA was found to be polysome-associated in the 4th instar PSG as compared to 90% in the 5th instar. Furthermore, the amount of fibroin H protein in the 4th instar was much lower than the expected synthesis from 40% of the polysome-associated mRNA. Thus, the operation of translational regulation of fibroin H synthesis was evident.

A possible reason for the translational block could be the limitation in supply of aminoacyl tRNAs in sufficiently large quantities and this aspect was therefore studied in detail. Chapter 4 presents a study on the levels of individual tRNA species and their cognate synthetases in the 4th and 5th instar PSG. A rapid and sensitive HPLC method was developed to quantitate the individual tRNA and their synthetases[7]. The method comprises (i) aminoacylation of total tRNA with (^{14}C) algal protein hydrolysate using homologous, partially purified total tRNA synthetase preparation, (ii) deacylation and recovery of (^{14}C) amino acids from charged tRNA, (iii) derivatisation of (^{14}C) amino acids in the presence of cold amino acids with phenylisothiocyanate, (iv) HPLC, to yield base-line separation of ptc-amino acids using volatile solvents, and (v) determination of radioactivity due to (^{14}C) amino acid in the individual amino acid peaks collected based on absorbance which directly corresponds to the amount of specific tRNA present in total tRNA fraction. The levels of aminoacyl tRNA synthetases were also determined under appropriate assay conditions.

Results of tRNA quantitation studies showed that in the 5th instar there was a dramatic increase in the levels of tRNA for Gly, Ala, Ser and Tyr and their synthetases while no such increase was observed in the PSG of the 4th instar. These results suggested that though the mRNA is polysome associated it cannot be translated efficiently in the 4th instar PSG due to the limited availability of tRNA species specific for fibroin H mRNA codons.

4. Determination of the modified base 5-methylcytosine in the developing silk glands

A rapid and sensitive method of repeating cycles of reverse-phase HPLC was developed for trace analysis, with a sensitivity of detecting 0.001 mol per cent of 5mC in DNA[8]. This method has a potential application in the determination of modified bases in DNAs from other systems.

The base analysis studies revealed that 5mC was present as a low-abundance base in PSG and MSG DNA. Its level increases by 17 and 15% in PSG and MSG, respectively, as the larvae progress from 4th to 5th instar. It is inferred that the increased methylation seen in the 5th instar gland may correspond to the transcriptional inactivation of non-silk proteins.

References

1. GOLDSMITH, M. R. AND KAFATOS, F. C. — *A. Rev. Genet.*, 1984, **18**, 443–487
2. AKAI, H. — *Experientia*, 1983, **39**, 443–449.
3. STRYDOM, D. J., HAYLETT, T. AND SEFID, R. H. — *Biochem. Biophys. Res. Commun.*, 1977, **79**, 932–938
4. TSUDA, M. AND SUZUKI, Y. — *Proc. Natn. Acad. Sci. USA*, 1983, **80**, 7442–7446.
5. MAEDA, R., KAWAKAMI, M. AND SHIMURA, K. — *J. Biochem.*, 1975, **78**, 391–400.
6. SUZUKI, Y. AND BROWN, D. D. — *J. Mol. Biol.*, 1972, **63**, 409–429.
7. PATEL, C. V. AND GOPINATHAN, K. P. — *Biochem. Biophys. Res. Commun.*, 1987, **142**, 334–340.
8. PATEL, C. V. AND GOPINATHAN, K. P. — *Anal. Biochem.*, 1987, **164**, 164–169.

Thesis Abstract (Ph.D.)

Regulation of expression of the genes coding for D-Ribulose, 1, 5, bisphosphate carboxylase/ oxygenase in callus and differentiating callus cultures of *Santalum album L.* by Girish N. Nallur.
Research supervisor: M. S. Shaila.
Department: Microbiology and Cell Biology.

1. Introduction

The plant enzyme D-Ribulose, 1-5, bisphosphate carboxylase/oxygenase (rubisco) is an important regulatory enzyme of the Calin cycle of photosynthesis. In higher plants, the enzyme is localized in the chloroplast matrix and is composed each of eight large subunits (LS) and small subunits (SS). The polypeptides vary in M_r between 52 and 55 K in different species while the SS polypeptides range between 12 and 15 K. The LS is encoded in the chloroplast genome and its mRNA is translated in the chloroplast matrix. The SS is encoded in the nuclear genome and its mRNA is translated on cytoplasmic ribosomes to yield a precursor (pSS) of M_r about 2000 d larger than the mature polypeptide. The pSS enters the chloroplast post-translationally and is concomitantly processed to its mature size and phosphorylated. The assembly of the LS polypeptides with the SS polypeptides occurs in the chloroplast matrix.

In green plants, the regulation of expression of the genes for rubisco is controlled primarily by

light *via* the photoreceptor phytochrome. The effect of light is to induce transcription of the SS gene and increase the copy number of the chloroplast genome. The amount of rubisco in leaves grown under bright illumination is about thirty fold over etiolated controls. Light also affects the activation state of the enzyme in leaves.

The assembly of rubisco within the chloroplast involves the function of another abundant protein termed the large subunit-binding protein (LSBP). The nuclear-coded LSBP protein is composed of two dissimilar subunits α and β of molecular weight 61 and 60 K, respectively. Newly synthesized LS polypeptides are bound non-covalently to this protein and in the presence of Mg ATP, get transferred to the SS polypeptides during assembly.

The activity of rubisco is modulated by phosphorylation in some plants. Also, a light-modulated phosphorylated inhibitor has recently been shown to maintain the right form of rubisco in an inactivated state. This inhibitor has been purified.

Although rubisco has been the subject of intensive investigation in higher plants, comparatively very little is known about the expression of rubisco genes in undifferentiated systems. In the present study, the mode of regulation of expression of rubisco genes has been studied in undifferentiated cells of *Santalum album* with a view to understanding the factors affecting such expression.

2. Experimental

Young stem explants of *Santalum album* were used to induce callus cultures. The callus was propagated on a medium consisting of Murashige and Skoog (MS) basal medium 1 supplemented with 5 ppm of 2,4-D. Gibberellic acid (GA_3) was used for differentiation of the calli and the medium used was Ms basal supplemented with 2 ppm of gibberellic acid.

The content of DNA, RNA and protein was measured in the callus and differentiating cultures at various periods. The DNA content was seen to increase in differentiating cells during the onset of differentiation and in callus just before the logarithmic phase of growth. There were two distinct phases of RNA and protein accumulation in callus while in differentiating cells, there was a single phase of increase in contents of these macromolecules following the phase of DNA accumulation. Differentiating cells showed significant rubisco activity after eight days in culture, while callus of any age totally lacked rubisco activity.

Rubisco was purified from leaves of *Santalum album* by two independent procedures, namely, ultracentrifugation[2] and fast-protein liquid chromatography[3]. The physical and kinetic properties of the enzyme studied compared well with those reported for the enzyme from other higher plants. Specific antiserum against purified rubisco was prepared and characterized.

3. Results and conclusions

The control of expression of the genes for rubisco in callus and differentiating cells was studied to explain the reason for the inactivity of callus rubisco. Using cloned-DNA probes specific for the SS and LS genomes, the two types of mRNA from callus and differentiating cells of various periods of growth were quantitated. The RNAs were seen to accumulate to comparable levels in both callus and differentiating cells. The qualitative features of the two classes of mRNAs were also similar in callus and differentiating cells. Using the cognate antibody, the presence of LS and SS polypeptides was identified from both callus and differentiating cells.

The lack of rubisco activity in extracts of callus cells could be due to a lack of assembly of the subunits into enzyme in these cells. However, this was found not to be so after the enzyme was

identified and quantitated from callus and differentiating cells. The presence of large subunit binding protein (LSBP) in callus cells was demonstrated which suggested that the assembly of enzyme in callus cells proceeded normally. The possibility that the enzyme was maintained in the inactive state due to phosphorylation or inhibitor binding was ruled out by appropriate investigation. The data suggest that the inactivity of rubisco from callus may be due to the LS subunit being synthesised in these cells as a precursor. The inability of the callus tissue to process the precursor to its mature size may be one of the reasons for the lack of enzyme activity of the assembled enzyme in the callus tissue. This processing activity appears in 16-day-old differentiating tissue, at which time, the rubisco enzyme activity is also seen.

References

1. MURASHIGE, T. AND SKOOG, F. *Physiol. Plantarum*, 1962, **15**, 473–497.
2. BERHOW, M. A., SALUJA, A. AND MCFADDEN, B. A. *Pl. Sci. Lett.*, 1982, **27**, 51–57.
3. BRIAT, J. F., LALLHERE, J. P. AND MACHE, R. *Eur. J. Biochem.*, 1979, **98**, 285–292.

Thesis Abstract (Ph.D.)

Toxicity and metabolism of R-(±)-pulegone in rats: Its effects on hepatic cytochrome P-450 *in vivo* and *in vitro* by B. Moorthy.
Research supervisors: K. M. Madyastha and C. S. Vaidyanathan.
Department: Organic Chemistry.

1. Introduction

Monoterpenes occur widely in nature and are used extensively as flavoring agents, fragrance component and also in pharmaceutical preparations, etc. Pulegone, a monoterpene ketone is the major constituent of pennyroyal oil from *Mentha pulegium*. In addition to its use as a flavoring agent, it has also been used as an abortifacient compound. A number of compounds including monoterpenes have been shown to induce the level of liver microsomal cytochrome P-450[1,2]. In our laboratory, we have shown that pulegone destroys hepatic cytochrome P-450 to a significant extent[3]. In the present investigation the toxicity and metabolism of R-(±)-pulegone in rats has been studied.

2. Material and methods

R-(±)-pulegone, menthone, carvone and aminopyrine were obtained from Aldrich Chem. Terpenoids were purified on silica gel column and distilled before use, piperonyl butoxide and diethyl maleate were obtained from Fluka. Phenobarbital (PB), 3-methylcholanthrene (3-MC), NADPH, NADH, cytochrome *c*, dilaurylphosphatidyl choline were obtained from Sigma. All other chemicals used were of analytical grade.

Microsomes were prepared from liver and kidney by a differential centrifugation method[4]. Cytochrome P-450 cytochrome b_5 cytochrome *c* reductase activities, heme content, protein, serum glutamate pyruate transaminase (SGPT), glucose-6-phosphatase and aminopyrine-N-demethylase

were determined as cited[5] Light and electron microscopic studies were conducted according to standard techniques. Urinary metabolites were isolated and purified by column chromatography and characterized by spectroscopic methods. *In vitro* destruction of cytochrome P-450 by pulegone and other compounds was performed as reported[3]. ^{14}C-pulegone was synthesized essentially according to the method of Black *et al*[6]. Covalent binding of ^{14}C-pulegone to microsomal proteins was assayed as described[7].

3. Results and discussion

Oral administration of pulegone to rats once daily for five days resulted in ~ 85% distribution of cytochrome P-450 and heme. Cytochrome b_5 and NAD(P) H cytochrome *c* reductase activities were not affected. Intraperitoneal administration of a single dose of pulegone (300 mg kg) resulted in 67% destruction of liver microsomal cytochrome P-450 and 31% loss in heme. Aminopyrine-N-demethylase and glucose-6-phosphatase level were also decreased significantly There was also a significant increase in the level of SGPT. This shows that pulegone is a potent hepatatoxin. The toxicity of pulegone was both dose and time dependent. Toxicity was potentiated by phenobarbital and diethylmaleate and protected by 3-methyl cholanthrene and piperonyl butoxide. This suggested the formation of a PB-induced cytochrome P-450 catalysed reactive metabolite of pulegone which could be responsible for the hepatotoxicity caused by pulegone.

Light microscope studies showed severe centrilobular necrosis of the liver in addition to periportal and midzonal and other degenerative charges. Electron microscope studies have shown severe damage to the endoplasmic recticulum and swelling of mitochondria. The changes were time dependent.

In vivo metabolism of pulegone in rats was investigated and six metabolites were isolated, *viz*., pulegol, 2-hydroxy-2(1'-hydroxy 1'-methylethyl)-5-methyl cyclohexanone, 3, 6-dimethyl-7a-hydroxy-2, 4, 5, 6, 7, 7a-hexahydrobenzofuran-2-one, menthofuran, 5-methyl-2(1'-methyl 1'-carboxyethylidene) cyclohexanone and 5-hydroxy-5-methyl-2 (1'-hydroxy 1'-carboxyethyl) cyclohexanone[8].

In vitro studies have clearly demonstrated that pulegone causes significant destruction of cytochrome P-450 and heme. The destruction of cytochrome P-450 was independent of metabolic activation. Destruction was more pronounced with PB-induced microsomes when compared with 3-methyl-cholanthrene-induced or control microsomes. The destruction of cytochrome P-450 was time dependent, saturable and followed first-order kinetics Destruction was prevented in the presence of SKF-525 A. A score of compounds structurally related to pulegone were tested for their ability to destroy cytochrome P-450 and the results have suggested that an α-isopropylidene ketone as seen in pulegone is necessary for the *in vitro* destruction of cytochrome P-450. Pulegone also caused significant destruction of purified cytochrome P-450 and caused an equimolar loss of heme.

Synthesis of ^{14}C-pulegone was accomplished and pulegone was shown to be covalently bound to the heme moiety. Incubation of ^{14}C-pulegone with liver microsome in the presence of NADPH resulted in covalent binding of pulegone to microsomal proteins. Covalent binding was higher with PB-induced liver microsomes. Covalent binding was drastically inhibited by piperonyl butoxide, cysteine, semicarbazide and antibodies to cytochrome P-450 and NADPH-cytochrome P-450 reductase. An α, β unsaturated aldehyde seems to be responsible for covalent binding to microsomal proteins.

In conclusion, it can be stated that pulegone not only exerts its destructive effect on cytochrome P-450 but also acts as a potent hepatotoxin. Both toxication and detoxication mechanisms seem to be operating during the metabolic process of pulegone in rats.

References

1. CINTI, D. L., LEMELIN, M. A. AND CHRISTIAN, J. — *Biochem. Pharmacol.*, 1976, **25**, 100–103
2. CHADA, A. AND MADYASTHA, K. M. — *Xenobiotica*, 1984, **14**, 365–374.
3. MADYASTHA, P., MOORTHY, B., VAIDYANATHAN, C. S. AND MADYASTHA, K. M. — *Biochem. Biophys. Res. Commun.*, 1985, **128**, 921–927.
4. RYAN, D., LU, A. Y. H. AND LEVIN, W. — *Methods Enzymol.*, 1978, **52**(C), 117–123.
5. MOORTHY, B., MADYASTHA, P. AND MADYASTHA, K. M. — *Toxicology*, 1989, **55**, 327–337
6. BLACK, C., BUCHANAN, G. L. AND JARVIE, A. W. — *J. Chem. Soc.*, 1956, 2971–2973.
7. MADYASTHA, K. M. AND MOORTHY B. — *Chem. Biol. Interactions*, 1989, **72**, 325–333.
8. MOORTHY, B., MADYASTHA, P. AND MADYASTHA, K. M. — *Xenobiotica*, 1989, **19**, 217–224.

Thesis Abstract (Ph.D.)

Copper(I)-promoted allylic nucleophilic substitutions: A synthetic and mechanistic study by J. B. Baruah.
Research supervisor: A. G. Samuelson.
Department: Inorganic and Physical Chemistry.

1. Introduction

Transition metal catalysts are used for regio- and stereoselective allylic nucleophilic substitution reactions[1-4] which are not possible in a classical organic reaction. Ancillary ligands, solvents, counter ions attached to the metal complexes modify the reactivity for such regio- and stereoselective transformations. Palladium complexes are extensively used for such transformations. In the present work, promotion of such reactions by copper(I) complexes was investigated.

The reaction described can be represented by Equation 1.

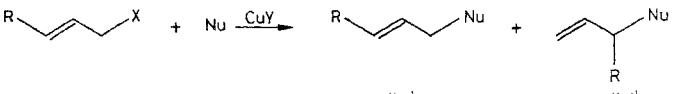

where R = Substituent; Nu = Nucleophile; Y = Anion attached to copper and X = Nucleofuge.
EQUATION 1

2. Results and discussion

Copper(I) perchlorate generated from copper metal powder and copper(II) perchlorate hexahydrate can very effectively promote the reaction between cyclic and acyclic allylic substrates with various

leaving groups towards nucleophilic substitution (Scheme I). The leaving groups studied were halides, acetates, carbonates, trifluoroacetates and alcohols. Nucleophilic substitution on allylic alcohols in a one-pot reaction was also achieved.

Alcohols reacted with allylic substrates giving corresponding allyl ethers. Regiochemical studies showed that alcohols led to attack at the more substituted end. Copper(I) chloride also could be used for these reactions.

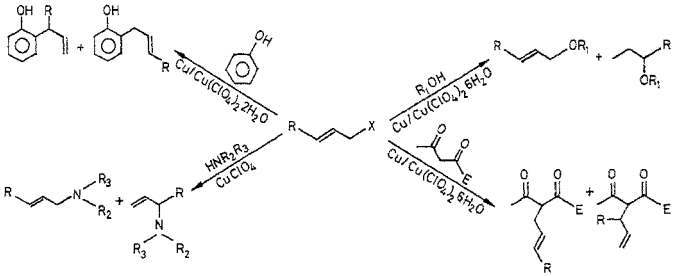

where R_1, R_2, R_3, R are alkyl or aryl groups and E = Ph, Me, OMe, OEt.

SCHEME I.

However, distinct differences in the regiochemistry of the attack of alcohols were observed. Surprisingly, reactions of phenols with allylic halides gave only C-allylated *ortho*allyl phenols. Aminations of allylic halides in the presence of copper(I) perchlorate showed that the ratios of α and γ attack depend on the size of the amine used. Various active methylene compounds reacted with allylic substrates in the presence of copper(I) perchlorate leading to attack at the less-hindered side.

Different copper salts of non-coordinating anions such as borontetrafluoride, trifluoromethane sulphonate could do such transformations. These reactions showed differences in α and γ attack when counter ions were different. The ratios of the products obtained in these reactions were also different from the Ag $\pm$ -promoted reactions.

To explain these results, deuterium labelling experiments were carried out using derivatives of *cis*-3-D-allyl alcohol (Fig. 1). The products analysed from various copper(I)-promoted nucleophilic substitution reactions have shown that a symmetric intermediate is involved. The reaction of benzyl alcohol with *cis*-3-D-allyl chloride showed the retention of double-bond geometry, whereas in the reaction of benzyl alcohol with *cis*-3-D-allyl acetate at a higher temperature rotation around the double bond was observed. Rotation around double bonds was observed in the reactions of geranyl acetate and neryl acetate with methyl acetoacetate in the presence of copper/copper(II) perchlorate hexahydrate. The stereochemistry of the carbon undergoing substitution was determined by using *cis* and *trans* carvyl acetate (Figs 2 and 3). Only the *trans* derivatives were formed in these reactions.

The mechanistic aspect of the reaction was studied by investigating the interactions of allyl benzoate with copper(I) perchlorate. Various other control experiments include scanning electron micrographic studies of copper metal powder during the course of the reaction, radical trapping experiments, reactions of cyclopropyl bromide and cyclopropyl carbinyl bromide with copper(I), propargyl bromide reaction with benzyl alcohol in the presence of copper(I), and attempts for optical induction using

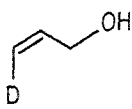

FIG 1.

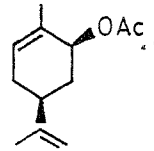

FIG 2

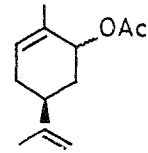

FIG 3.

a copper(I) complex of (+) cinchonine, reaction of homoallylic bromides with alcohols in the presence of Cu Cu $(ClO_4)_2 6H_2O$. From these control experiments it became evident that the reaction took place through an initial complexation of allylic substrate to copper(I) (Scheme II). The olefin copper(I) complex oxidatively adds to allylic substrates which could be the rate-determining step as the rate

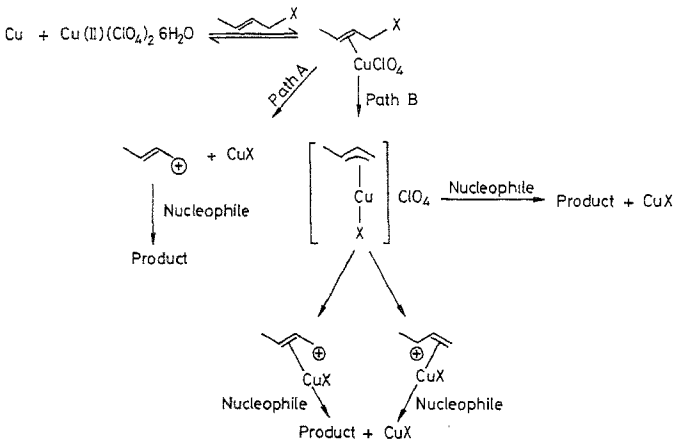

SCHEME II.

of reaction varies in the order Br > Cl > OAc > OH. The π-allyl complex thus formed could give the substitution reaction or could break down to a coordinated cation or a free cation to give the products.

3. Conclusion

These results suggest that results similar to those in the palladium-catalysed allylic nucleophilic substitutions could be achieved with copper(I) complexes under appropriate conditions. Copper(I)-promoted allylic nucleophilic substitution reaction was carried out in neutral or slightly acidic conditions which has advantages over much widely used palladium-catalysed reactions where a basic medium is necessary.

References

1. BOSNICH, B AND MACKENZIE, P. B. *Pure Appl. Chem.*, 1982, **54**, 189–196
2. TROSTM, B. M. AND VERHOEVEN, T. R *J. Am. Chem. Soc.*, 1980, **102**, 4730–4743.
3. TSUJI, J. *Pure Appl. Chem.*, 1982, **54**, 197–206.
4. SILVERMAN, G. S., STRICKLAND, S. AND NICHOLAS, K. M. *Organometallics*, 1986, **5**, 2117–2124

Thesis Abstract (Ph.D.)

Studies on fine particle alpha alumina and related oxides prepared by a novel combustion process by J. Jawahar Kingsley.
Research supervisor: K. C. Patil.
Department: Inorganic and Physical Chemistry.

1. Introduction

Aluminous oxides form one of the major and most important class among oxide ceramics. Their technological applications[1] as refractories, abrasives, cutting tools (α-Al_2O_3, $MgAl_2O_4$), high alumina cement ($CaAl_2O_4$), catalyst ($LaAlO_3$. $CuAl_2O_4$), lasers (Ruby, Cr^{3+}/Al_2O_3, $Nd^{3+}/Y_3Al_5O_{12}$, Nd: YAG), TV phosphors ($Ce^{3+}/CaAl_{12}O_{19}$), pigments ($CoAl_2O_4$), solid electrolytes in Na-S batteries (β-alumina), toughened ceramics (t-ZrO_2/Al_2O_3) and in fluorescent lamps ($Ce^{3+}/Y_3Al_5O_{12}$, $CeMgAl_{11}O_{19}$) make them really more attractive and useful.

The conventional ceramic method of preparing these oxides involves solid-state reaction of the component oxides at elevated temperatures (1000–1600°C) over an extended period. The products obtained from this process are quite inhomogeneous and show poor reactivity as the product oxides are hard agglomerates (large particles). Several wet chemical methods[2] such as coprecipitation, pyrolysis of metal salt solutions, spray-drying, sol-gel process, etc., have been employed to prepare reactive fine powders of these oxides. Nevertheless, they are involved and require high temperatures (> 1000°C) and long time.

Self-propagating high-temperature synthesis (SHS or SPS) method[3] involving metal powders (Ti, Zr, Ta, etc.) and non-metals (C, B, Si, etc.) has been employed for the preparation of exotic high-temperature ceramics such as metal carbides, borides, silicides which find applications as refractories, abrasives, heating elements and in powder metallurgy. It is interesting to note that the exothermicity of these solid-state reactions arises from the chemical reaction between metals and non-metals which act as fuels and oxidisers, respectively. Extending this idea it has now been possible to prepare α-Al_2O_3 and related oxide materials using metal nitrates as oxidisers and urea/carbohydrazide as fuels.

2. Experimental

Techniques used in the present study are simultaneous thermal analysis, surface area measurement, particle size analysis, X-ray powder diffraction, electron microscopy (SEM, TEM, HREM and EPMA),

fluorescence spectroscopy, UV-Vis spectroscopy, electron spin-resonance spectroscopy and pulsed laser decay time measurement.

3. Results and discussion

3.1. *Combustion synthesis and properties of fine-particle alpha alumina*[4]

Combustion of aluminium nitrate-urea (1:2.5) mixture when heated rapidly at 500°C_2, boils, froths, foams and ignites to burn with incandescence (flame temperature of ~ 350°C) to yield fine, fluffy and voluminous α-Al_2O_3 in 5 minutes under normal atmospheric pressure. Formation of single-phase α-Al_2O_3 (the high-temperature form) was confirmed by its X-ray powder diffraction pattern and the fine particle nature of the product has been investigated by surface area measurement and particle size analysis. The product (α-Al_2O_3) has a foam density of 9.06×10^{-3} g/cm^3 and a tap density of 0.06 g cm^3 The surface area of the as-prepared α-Al_2O_3 was 8.3 m^2/g with particle size ranging from 0.2 to 0.8 μm. The average agglomerate size of α-Al_2O_3 is 4.3 μm.

3.2. *Combustion synthesis and properties of fine-particle t-ZrO_2/Al_2O_3*

The combustion of zirconyl nitrate-aluminium nitrate-urea mixtures yields *t*-ZrO_2/Al_2O_3 composite powders having uniform distribution of tetragonal zirconia in α-Al_2O_3 as evidenced by its X-ray diffraction pattern and electron microscopic analysis (SEM, TEM, HREM and EPMA). The crystallite size of *t*-ZrO_2 is below 300 Å as required for its stabilization. The inhibited coarsening observed on these composites is of special relevance in these metastable *t*-ZrO_2/Al_2O_3 composites.

3.3. *Combustion synthesis and properties of fine-particle metal aluminates*[5]

Fine-particle metal aluminates, MAl_2O_4 where M = Mg, Ca, Ba, Sr and Zn, $Ca_3Al_2O_6$ and calcium hexaaluminate, $CaAl_{12}O_{19}$ have been prepared by the combustion of corresponding metal nitrates-aluminium nitrate-urea mixtures at 500°C within 5 minutes.

Metal aluminates, MAl_2O_4 where M = Mn, Co, Ni and Cu which could not be obtained by urea process have been prepared by the combustion of corresponding metal nitrate-aluminium nitrate-carbohydrazide mixtures at 350°C. The surface area of metal aluminates prepared by carbohydrazide process was higher (40–80 m^2/g) compared to those obtained by urea process (1–2 m^2/g). It was also possible to prepare β, β' alumina using the combustion of aluminium nitrate-sodium nitrate-urea mixtures at 500°C. The formation of single-phase aluminates was confirmed by the characteristic X-ray powder diffraction patterns and their fine particle nature was studied by SEM, TEM, particle size and surface area analysis.

3.4. *Combustion synthesis and properties of fine-particle rare-earth orthoaluminates and yttrium aluminium garnet*[6]

Rare-earth orthoaluminates, $LnAlO_3$, where Ln = La, Pr, Nd, Sm, Gd, Tb and Dy and yttrium aluminium garnet, $Y_3Al_5O_{12}$(YAG) have been prepared by the combustion of corresponding rare-earth nitrates-aluminium nitrate-urea/carbohydrazide mixtures at 500°C. These as-prepared oxides were fine with the particle size in the range of 0.1–0.6 μm with an average agglomerate size of 4–5 μm.

3 5. *Combustion synthesis and properties of fine-particle fluorescent aluminous oxides*"

The instant combustion process developed for the preparation of α-Al_2O_3, metal aluminates and rare-earth orthoaluminates has been extended to the preparation of fine-particle fluorescence aluminous oxide materials like Cr^{3+}-doped α-Al_2O_3 (Ruby), $MgAl_2O_4$, $LaAlO_3$, $Y_3Al_5O_{12}$ and Ce^{3+}-doped $Y_3Al_5O_{12}$, $LaMgAl_{11}O_{19}$ and $CaAl_{12}O_{19}$. Formation of these Cr^{3+}- and Ce^{3+}-doped aluminous oxides has been confirmed by their characteristic colour, UV-visible and fluorescence spectra and decay time measuements. Ruby (Cr^{3+}/α-Al_2O_3) powder showed the characteristic excitation bands at 406 and 548 nm and emission band at 695 nm with the decay time of 3.6 ms.

References

1. GITZEN, W. H. (ed.)	*Alumina as a ceramic material*, 1970, The American Ceramic Society, Inc
2 ROETTENBACHER, R. AND SCHMIDBERGER, R.	*Ceramic powders*, in *Materials Science Monographs* (P. Vincenzini ed.), Vol 16, 1983, p. 539, Elsevier.
3 KOVALYOVA, A	Materials born in fire, *Sci. USSR*, 1988, **2**, 44–47.
4 KINGSLEY, J J AND PATIL, K. C.	A novel combustion process for the synthesis of fine particle α-alumina and related oxide materials, *Mater. Lett.*, 1988, **6**, 427–432.
5 KINGSLEY, J J., SURESH, K AND PATIL, K. C.	Combustion synthesis of fine particle metal aluminates, *J. Mater. Sci.*, 1990, **25**, 1305–1312.
6. KINGSLEY, J J. SUNDER MANOHARAN, S AND PATIL, K. C.	Combustion synthesis of rare earth orthoaluminates, chromates and yttrium aluminum garnets, *Ist Indo-Soviet Seminar on rare earth and actinide compounds*, Tallinn, USSR, Sept. 19–21, 1988.
7 KINGSLEY, J. J., MANICKAM, N. AND PATIL, K. C	Combustion synthesis and properties of fine particle fluorescent aluminous oxides, *Bull. Mater. Sci.*, 1990, **13**, 179–189.

Thesis Abstract (Ph.D.)

Sacrificial water photolysis on TiO_2 and $SrTiO_2$ fine powders under band-gap irradiation

by M. Avudaithai.
Research supervisor: T. R. N. Kutty.
Department: Inorganic and Physical Chemistry.

1. Introduction

The conversion of solar energy at the semiconductor/electrolyte junctions is based either on the photoelectrochemical cells which incorporate the bulk semiconductor electrodes[1] or on the semiconductor fine powder photocatalysis[2]. In photocatalysis, electrons and holes are generated on band-gap irradiation of the semiconductor fine powders and are separated by the electric field at the interface. These species migrate to the semiconductor surface and involve themselves in the redox reactions. There have been many approaches to the conversion of photon energy into chemical energy. One of the attractive routes is the photodecomposition of H_2O into H_2 and O_2 using semiconductor materials. However, efficient decomposition of H_2O using solar irradiation has been less successful. Efforts are on to find new semiconductors with proper band gap to match the maximum in the solar

spectrum and which do not undergo photo-corrosion or degradation. The problem is to either improve the efficiency of the large band-gap materials or to avoid corrosion of small band-gap semiconductors. The aim of the present investigation is to understand the photocatalytic behaviour of TiO_2 and $SrTiO_3$ fine powders in the presence of reducing agents. The study has been restricted to bulk and surface modifications of these powders to explain the controversial results reported in literature[3,4] and to achieve higher hydrogen evolution efficiencies.

2. Experimental

TiO_2 and $SrTiO_3$ fine powders are prepared by hydrothermal method. Fine powders of TiO_2 (rutile) with high degree of crystallinity are formed from $TiOCl_2$ at 160–230°C and at 20–120 atm[5]. The anatase phase is produced from the same mixture when sulphate ion impurity is present with $[SO_4^{2-}]/[Cl^-] \geq 0.03$. $Ti_{1-x}Sn_xO_2$ solid solution, where $0 < x < 1$, is prepared at 220–250°C from the coprecipitated hydroxides of $TiOCl_2$ and $SnCl_4$ with NaOH or NH_4OH[6]. Similarly, TiO_2 fine powders substituted with different ions like Nb, Zr, etc., are also prepared by this method. Fine powders of $SrTiO_3$ are prepared at 120–150°C from $Sr(OH)_2$ and $TiO_2 \cdot 2H_2O$ gel[7]. Mixed solvent medium of H_2O–C_3H_7OH is used to get very fine powders.

Structural studies were carried out using X-ray powder diffraction techniques and paramagnetic trap centres are identified by EPR studies on a Varian E109 X-band spectrometer. Particle size measurement and electron diffraction studies were carried out using transmission electron microscope (Philips EM 301). The composition of electrode surface has been studied by XPS (Kratos 850). Instrumental techniques used for photoelectrochemical measurements involve cyclic voltammetry, current-voltage measurement and gas chromatography.

3. Results and discussion

The role of surface hydroxylation of TiO_2 particles as an essential characteristic for their photocatalytic activity is verified by hydrothermally prepared TiO_2 powders since hydroxylated surface layers are better retained on these particles formed under super-heated H_2O[5]. Both rutile and anatase fine powders do not yield detectable amount of H_2, either in the as-prepared form or after loading with Pt, whereas H_2 is detected in the presence of hole scavengers such as EDTA, TEOA, sulphite or hypophosphite. The fact that the metal loading of TiO_2 does not induce photocatalytic activity in systems without hole scavengers may indicate the rapid electron-hole recombination in fine TiO_2 particles. Recombination can be retarded by the hole scavenger which is in close proximity to TiO_2 by way of surface adsorption. From this it is clear that H_2 does not arise from the surface hydroxyl groups on TiO_2 during water photolysis. A critical value of hole-scavenger concentration, Pt: TiO_2 ratio and particulate suspension density were observed for the maximum H_2 production. Platinized rutile powders are equally active as anatase in the sacrificial system.

Paramagnetic trap centres are formed in the TiO_2 particles during water photolysis at room temperature[8] under band-gap irradiation. Irradiation of TiO_2 fine powders dispersed in water gives rise to both electron and hole centres, whereas only the hole centre is observed on irradiation of platinized TiO_2 powder dispersed in water. This shows that the electrons produced on irradiation are involved in H_2 production. In the presence of hole scavenger only the electron centre is observed which indicates the abstraction of holes by donor molecules. The trapped holes corresponding to O^- species adjacent to the cation vacancies and the trapped electrons are accounted as Ti^{3+} adjoining the oxygen vacancy to form Ti^{3+}–V_O–Ti^{4+} shallow donor states. Although hole centres are normally more stable than the electron centres, strongly adsorbed donor molecules reverse the stability. Concentration of hole centres increases in the presence of Pt on TiO_2 surface which explains the low

O_2 yield obtained by many authors in water photolysis using Pt/TiO_2. Although hole and electron trap centres are produced in TiO_2 during UV irradiation of the particle dispersions in water at room temperature, they are detectable by EPR only at low temperatures due to spin-lattice relaxation. Reactivity of trapped holes is lower than that of trapped electrons.

$Ti_{1-x}Sn_xO_2$ solid products, when oven-dried, are pale yellow[6]. EPR results show that the yellow colour is not due to transition metal impurities. Yellow colour is also observable using NaOH in place of NH_4OH showing that it does not arise from NO_2 doping. Spectral sensitization is shown to be due to peroxotitanium species in the rutile-type structure. Peroxide O_2^{2-} arises from the dimerization of O^-, which are the hole centres produced during the disproportionative decomposition of residual hydroxyls: $OH^- = O^- + H$. These powders show photocatalytic activity after platinization in the visible region (420–550 nm) from aqueous solutions containing sacrificial donors such as hypophosphite. The rate of H_2 production increases with Sn content up to $x = 0.35$ and decreases at higher x values. Introducing anionic species such as O_2^{2-} in $Ti_{1-x}Sn_xO_2$ may be useful to increase the visible light response of wide band-gap oxides.

H_2 production is observed in the presence of a hole scavenger such as EDTA on band-gap irradiation of TiO_2; Nb powder, after Pt loading. H_2 evolution capacity of TiO_2 enhances only up to a limited compositional range of 0.3 mole % Nb. At higher Nb content, H_2 yield decreases far below the value for undoped rutile. EPR investigations indicate that the electron centres stable under ambient conditions are: Nb_{Ti}^{4+}–V_0–Ti^{4+} or Ti^{3+}–V_0–Ti^{4+}, where the electron trapped at the oxygen vacancy has partial residence at the contiguous Nb^{5+} or Ti^{4+} ions. EPR results also show that the electron centres are more populated during the sacrificial photolysis where the hole centres vanish. Photocatalytic activity of Zr^{4+} and various aliovalent ion-substituted TiO_2 powders are studied. $Ti_{0.9}Zr_{0.1}O_2$ has nearly the same activity in all the hole scavengers (EDTA, H_2PO_2 and TEOA). Though the undoped TiO_2 has the highest activity in EDTA, 1% metal ion (Al^{3+}, Fe^{3+}...) incorporation decreases the activity in EDTA tremendously.

Aqueous suspensions of $SrTiO_3$ powders do not produce H_2 or O_2 on UV irradiation. H_2 and O_2 are evolved on UV illumination after coating with Pt or Rh[6] but the yield is very low. However, appreciable amount of H_2 production is noticed in solutions containing $H_2PO_2^-$ as the hole scavenger. A critical value for the concentration of Pt mounting, dispersion density and $H_2PO_2^-$ concentration was observed for the maximum H_2 production.

EPR spectra of $SrTiO_3$ fine powders prepared by different routes vary considerably with respect to their background impurities and also of the native defect centres. The defect centres which participate in the charge-transfer process during photolysis could be identified from the EPR spectra of $SrTiO_3$ powders that are recovered after irradiation. The decrease in intensity of the hole-centre signal on irradiation of water suspension can be accounted in terms of hole transfer to H_2O leading to O_2 evolution whereas the intensity of the hole-centre signal in TiO_2 increases with irradiation time. This explains the observation of O_2 evolution only in the case of $SrTiO_3$. This signal disappears completely when the hydrothermal $SrTiO_3$ powder is irradiated in EDTA or $H_2PO_2^-$.

Various surface treatments such as grinding and etching only lowers the H_2 yield when compared to the untreated powder. To identify the defect (surface) states produced during surface treatments, TiO_2 bulk electrodes (sintered) are used since they are better amenable for electrochemical measurements than the powder systems. Surface states identified in the case of polished electrodes[9] can be extended to varying results reported in literature on the photocatalytic activity of the TiO_2 fine powders. Accumulation of electrons on polished electrodes explains the decrease in H_2 yield with the milled TiO_2 particles. Surface states related to peroxide ions also explain the O_2 evolution which is reported by some authors in the non-sacrificial water photolysis.

References

1 FUJISHIMA, A AND HONDA, K *Nature*, 1972, **238**, 37–38.

2 KIWI, J., KALYANASUNDARAM, K. AND GRATZEL, M *Struct. Bonding* (Berlin), 1982, **49**, 37–125.

3 MARUSKA, H P AND GHOSH, A K *Solar Energy*, 1978, **20**, 443–458.

4 JAEGER, C. D. AND BARD, A J *J Phys. Chem.*, 1979, **83**, 3146–3152.

5 KUTTY, T. R. N. AND AVUDAITHAI, M *Mater. Res. Bull.*, 1988, **23**, 725–734.

6. KUTTY, T. R. N. AND AVUDAITHAI, M. *Chem. Phys. Lett.*, 1989, **163**, 93–97.

7 AVUDAITHAI, M. AND KUTTY, T R N. *Mater. Res. Bull.*, 1987, **22**, 641–650.

8. AVUDAITHAI, M. AND KUTTY, T. R. N. *Mater. Res. Bull.*, 1988, **23**, 1675–1683.

9 KUTTY, T. R N., GOMATHI DEVI, L. AND AVUDAITHAI, M. *Solar Energy Mater.*, 1990, **20**, 307–321.

Thesis Abstract (Ph.D.)

Chemistry of spirocyclic compounds by P. Amruta Reddy.
Research supervisor: T. R. Kasturi.
Department: Organic Chemistry.

1. Introduction

Spirodienones, an interesting class of compounds which occur widely in nature and are important in biosynthesis, have a fascinating chemistry[1]. The term *spirodienone* is used in this context to describe derivatives of cyclohexa-2,4- and 2,5-dienones **1** and **2** in which carbon atoms 6 and 4 are spirocentres. Many natural products containing the spirodienone moiety and which could be derived from it are known in literature[2–6]. Oxidative phenolic coupling is an important method for the synthesis of spirodienones[7,8]. Several spironaphthalenones have been synthesised in this laboratory by DDQ/*O*-chloranil oxidation of naphthol derivatives[9].

An X-ray crystallographic investigation[10] of *cis* dispironaphthalenone **3a** showed that the C(2')–C(3') bond is unusually stretched (1.616 Å) and that the two olefinic π-bonds of the enones are fairly well oriented for intramolecular cycloaddition. Irradiation of **3a** in benzene using 450 w medium pressure mercury vapour lamp has resulted in the formation of a wide range of products **4a–6a**. To investigate the generality of this photoreaction and the effect of bulky substituents, if any, on the reaction, irradiation of a few dispironaphthalenones **3c–3d** was undertaken which resulted in the formation of quinonemethide dimers **4c**, **4d**, dinaphthodioxins **5b**, **5c** and intramolecular [π_2S + π_2S] cycloadducts **6b**, **6c**.

2. Results and discussion

Irradiation of the biallylic alcohol 7 gave only the (π_2S + π_2S] cycloaddition product **6d**. The quinonementhide dimers **4a–e**, on irradiation in the UV region surprisingly isomerised to thermo-

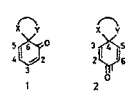

1 2 3 4 5

3
a: R = H
b: R = Br
c: R = Bu^t
d. R' =

4
a : R = R' = H
b : R = Br, R' = H
c : R = Bu^t, R' = H
d : R =  , R' = H
e : R = H, R' = Me

5
a : R = H
b : R = Bu^t
c : R = 

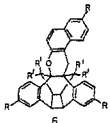

6
a: R = H, R' = =O
b: R = Bu^t, R' = =O
c: R =  , R' = =O ; d: R = H, R' = 

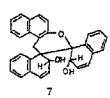

7

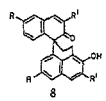

8
Substituents as in 4

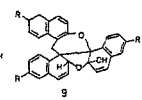

9
a : R = H
b : R = Br
c : R = Bu^t
d : R =

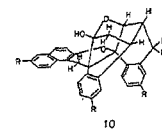

10
a : R = H
b : R = Br
c : R = Bu^t
d : R = 

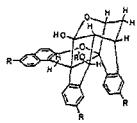

11
a: R = H, R' = Me
b: R = H, R' = Et
c: R = H, R' = Pr^i
d: R =  , R' = Me
e: R =  , R' = Et
f: R =  , R' = Pr^i

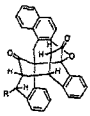

12
a: R = OMe
b: R = OEt
c: R = OPr^i
d: R = $CH(CO_2Me)_2$
e: R = $CH(CO_2Et)_2$

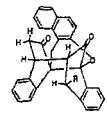

13
a: R = OMe
b: R = OEt
c : R = OPr^i

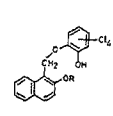

14
a : R = H
b : R = THP

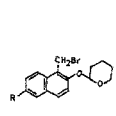

15
a : R = H
b : R = Br

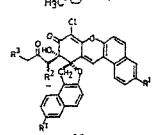

16
a : $R^1 = R^2 = R^3 = H$
b : R^1 = Br, $R^2 = R^3$ = H
c : R^1 = Br, R^2 = α-Me, R^3 = Me
d : $R^1 = R^2$ = H, R^3 = Me

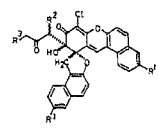

17
a: $R^1 = R^2 = R^3 = H$
b: R^1 = Br, $R^2 = R^3$ = H
c: R^1 = Br, R^2 = α-Me, R^2 = Me
d: R^1 = Br, R^2 = β-Me, R^3 = Me
e: $R^1 = R^2$ = H, R^3 = Me
f : R^1 = Br, R^2 = H, R^3 = Me
g: R^1 = H, R^2 = β-Me, R^3 = H
h: R^1 = Br, R^2 = β-Me, R^3 = H
i : R^1 = Br, R^2 = α-Me, R^3 = H

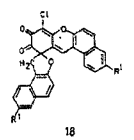

18
R^1 = H, Br

dynamically more stable phenolic phenalene derivatives **8a–e**. Structures of all these compounds are based on a detailed study of their spectral data. Formation of the unusual photoproducts has been explained *via* the initial β-C–C or β-C–O cleavage.

Sodium borohydride reduction of dispironaphthalenone **3a** in THF was found to give a novel intramolecular carbon-carbon coupled hemiacetal **10a** along with the hemiacetal **9a** and the biallylic alcohol **7**. It has also been shown that the $NaBH_4$ reduction of **3a** in alcohol–THF containing alkali gives structurally and mechanistically interesting novel intramolecular carbon-carbon coupled hemiacetals **11a–c** along with the hemiacetal **9c**. The generality of these reactions has been demonstrated by using different substrates **3b–d** to yield the corresponding products **9b–d**, **10b–d** and **11d–f**. As a consequence of this observation, addition of different oxygen and carbon nucleophiles to the dispironaphthalenone **3a** was studied when the diketones of the type **12** and **13** were isolated. $NaBH_4$ reduction of the diketone **12a** gave the known hemiacetal **11a**, thus confirming the structure assigned to this compound. Formation of the unusual products in the above reactions has been explained by Michael–Michael-type annelation process.

In connection with the mechanistic studies on the unusual oxidative rearrangement of substituted 2-naphthols and oxydiphenols[11], synthesis of the oxydiphenol **14a** was attempted by condensation of the bromide **15a** with tetrachlorocatechol in the presence of anhydrous potassium carbonate in acetone followed by removal of tetrahydropyranyl group of the resulting product **14b**. To investigate the structure of the unanticipated products in the above condensation reaction, it was repeated with bromide **15b**. The resulting quinonemethide dimer **4b** and novel diastereomeric polycylic aromatic compounds **16b** and **17b** were thoroughly characterized[12]. Accordingly, structures **16a** and **17a** were assigned for the products isolated in the reaction of bromide **15a**. A tentative mechanism proposed for the formation of the polycyclic compounds involves: (i) formation of 1,2-naphthoquinone-1-methide from the bromo compound, (ii) Michael addition of tetrachloro-catechol to quinone methide resulting in diketone **18**, and (iii) aldolisation of diketone with the solvent acetone. The base-induced cleavage of tetrahydropyranyl ether has been demonstrated by utilising different bases like Na_2CO_3, NaOMe and Et_3N in CH_3CN. Even though diketone **18** has not been isolated, the aldolisation step has been demonstrated by changing the solvent acetone to diethyl ketone or ethyl methyl ketone when the corresponding diastereomeric compounds of the type **16** and **17** were isolated. X-ray crystal structure analysis of compounds **16b** and **17b** confirmed the structures assigned to these two classes of compounds.

3. Conclusions

A novel one step method has thus been developed for the synthesis of polycyclic aromatic compounds. This could be utilised in the synthesis of biologically active compounds containing nitrogen in the ring system.

References

1. WARD, R. S. *Chem. Brit.*, 1973, 444–461.
2. CHOU, C. T. AND SWENTON, J. S. *J. Am. Chem. Soc.*, 1987, **109**, 6898–6899.
3. LUDWIG, W. AND SCHAFER, H. J. *Angew Chem.*, 1986, **25**, 1025–1026.
4. MARTÍN, S. F. AND DAVIDSEN, S. K. *J. Am. Chem. Soc.*, 1984, **106**, 6431–6433.
5. DANISHEFSKY, S., MORRIS, J., MULLEN, G. AND GAMMILL, R. *J. Am. Chem. Soc.*, 1982, **104**, 7591–7599.

6 DANISHEFSKY, S., MORRIS, J., MULLEN, G. AND GAMMILL, R. — *J. Am. Chem. Soc.*, 1980, **102**, 2838–2840

7. MUSSO, H. — *Phenol coupling in oxidative coupling of phenols*, (eds) Taylor, W. I. and Battersby, A. R., Marcel Dekker, pp 1–94.

8 THOMSON, R. H. — *Biochemistry of phenolic compounds*, 1964, pp 1–82, Academic

9. KASTURI, T. R. — *Proc. Indian Acad. Sci. (Chem. Sci.)*, 1984, **93**, 531–545

10. KASTURI, T. R., RAJASEKHAR B., RAJU. G. J., MADHUSUDHAN REDDY, G., SIVARAMAKRISHNAN, R., RAMASUBBU, N. AND VENKATESAN, K. — *J. Chem Soc., Perkin Trans. I*, 1984, 2375–2382

11. KASTURI, T. R., GANESH PRASAD, K. B. AND RAJASEKHAR, B. — *Indian J. Chem.*, 1982, **21B**, 813–818.

12. KASTURI, T. R., RAJASEKHAR. B., SIVARAMAKRISHNAN, R., AMRUTA REDDY, P., MADHUSUDHAN REDDY, G., GANESH PRASAD, K. B., VENKATESAN, K., GURU ROW, T. N., PURANIK, V. G. AND TAVALE, S. S. — *Indian J. Chem.*, 1986, **25B**, 1091–1092.